SMALL-LABS: An algorithm for measuring single-molecule intensity and

position in the presence of obscuring backgrounds

Benjamin P. Isaacoff, Yilai Li, Stephen A. Lee, and Julie S. Biteen* University of Michigan Department of Chemistry, Ann Arbor, MI 48104

*To whom correspondence should be addressed: jsbiteen@umich.edu

ABSTRACT

Single-molecule and super-resolution imaging relies on successfully, sensitively, and accurately

detecting the emission from fluorescent molecules. Yet, despite the widespread adoption of

super-resolution microscopies, single-molecule data processing algorithms can fail to provide

accurate measurements of the brightness and position of molecules in the presence of

backgrounds that fluctuate significantly over time and space. Thus, samples or experiments that

include obscuring backgrounds can severely—or even completely—hinder this process. To date,

no general data analysis approach to this problem has been introduced that is capable of

removing obscuring backgrounds for a wide variety of experimental modalities. To address this

need, we present the SMALL-LABS (Single-Molecule Accurate LocaLization by LocAl

Background Subtraction) algorithm, which can be incorporated into existing single-molecule and

super-resolution analysis packages to accurately locate and measure the intensity of single

molecules, regardless of the shape or brightness of the background. Accurate background

subtraction is enabled by separating the foreground from the background based on differences in

the temporal variations of the foreground and the background—fluorophore blinking, bleaching,

or moving. We detail the function of SMALL-LABS here and we validate this algorithm on

simulated data as well as real data from single-molecule imaging in living cells.

KEYWORDS. Super-resolution imaging, single-molecule microscopy, image processing,

nanoparticles, cellular biophysics.

Condensed Running Title: SMALL-LABS for obscuring backgrounds

1

Single-molecule super-resolution imaging has revolutionized microscopy (1–5) through a variety of experimental modalities, such as stochastic optical reconstruction microscopy (STORM) (6) photoactivated localization microscopy (PALM) (7, 8), and points accumulation for imaging in nanoscale topography (PAINT) (9). Yet, these experimental techniques all rely on accurately and precisely localizing single emitters with successful data processing algorithms (10–14). Realistic backgrounds vary in time and space and decrease the signal-to-noise ratio; these backgrounds can severely obscure super-resolution imaging by reducing the localization precision, introducing systematic biases, and even preventing successful detection through both false-positive and false-negative errors. In addition to improving single-molecule localization, a particular challenge in the field is to attain unbiased measurements of single-molecule intensities for single-molecule counting experiments, single-molecule fluorescence resonance energy transfer (FRET) experiments, and as a single-molecule probe of the local environment.

Experimental measures can certainly decrease backgrounds. However, popular methods for this purpose, such as confined illumination via light sheets (15–17) and total internal reflection (TIRF) (18), reduce out-of-focus fluorescence, but do not address in-plane backgrounds. Longer wavelength excitation decreases cellular autofluorescence (19), but sacrifices the resolution improvement of imaging at a shorter wavelength. Additional fluorescent objects incorporated into the sample for added functionality, such as plasmonic antennas for fluorescence enhancement or fiducial markers for drift compensation, improve imaging, but themselves produce a punctate spot in the background that can be misidentified as a fluorescent molecule (fluorophore) or that can obfuscate nearby fluorophores (20–22). Moreover, these adaptations tend to complicate or restrict experiments. As a broadly applicable alternative to modifying experimental designs to reduce backgrounds, we report here a general algorithm: SMALL-LABS (Single-Molecule Accurate LocaLization by LocAl Background Subtraction), which accurately locates and measures the intensity of single molecules, regardless of the shape or brightness of the background. Accurate background subtraction is enabled by separating the foreground from the background based on differences in the temporal variations of the foreground and the background due to fluorophore blinking, bleaching, or moving.

To our knowledge, no other background removal algorithm to date can eliminate the systematic bias in intensity measurements and position determination (localization) for a wide

range of experimental systems (Supplementary Note 1). For instance, though several new approaches can accurately localize single molecules within a dense ensemble (10, 11), these algorithms assume a background shaped like the image of an overlapping neighboring molecule and fail for arbitrary backgrounds. Additionally, such high-density approaches indiscriminately identify as molecules all signals that look like the system point spread function (PSF) regardless of the temporal dynamics. In general, approaches that attempt to subtract the background without first identifying the foreground (23) will inevitably introduce distortions by subtracting some of the image of a fluorophore from itself (Supplementary Note 2). SMALL-LABS provides the true background-subtracted image for single-molecule data by specifically distinguishing the foreground from the background; the only requirement is that the local background changes more slowly than the characteristic on/off timescale of the fluorophores. In this Computational Tools article, we present SMALL-LABS and detail its function, we validate its performance on simulated single-molecule fluorescence data, and we demonstrate its capability on measured live-cell single-molecule data. We also provide open-source Matlab code that implements the SMALL-LABS algorithm.

SMALL-LABS operating principles. The SMALL-LABS algorithm comprises a workflow described in detail below and summarized here. First, an *approximate background* calculated from the running average is subtracted from the raw movie, making single fluorescent molecules detectable with standard image analysis techniques (Step *I*; Fig. 1 *a* and *b*). This approximate background correction (23) removes the obscuring background, but will also subtract part of the true image from itself, reducing the apparent intensity and possibly introducing systematic biases (Supplementary Note 2). Therefore SMALL-LABS uses the approximate background subtraction only for this initial molecule detection step (Step *II*; Fig. 1 *b*). Next, for each detection, SMALL-LABS identifies which frames contained detections at or near the position of the current detection. Fluorophores can turn on and off due to blinking, bleaching, or moving, so this check produces a list of "off" imaging frames in which no other molecule is detected in the local vicinity of each detected molecule (Step *III*). The *true local background* is defined in SMALL-LABS as the average of these "off" frame images at the molecule position. Finally, this true background is removed locally for each detected ("on" frame) molecule (Step *IV*; Fig. 1 *c*).

Importantly, this algorithm does not subtract the image of a molecule from itself, ensuring that further analysis of the background-subtracted image provides accurate super-resolution information and avoids the systematic biases in the determination of each molecule's brightness that would arise from incorrect background subtraction (Step V).

The SMALL-LABS algorithm is described in this article. We also provide open-source code which implements this algorithm. The code we provide is customizable for diverse datasets (for details, see the User Guide), though optimized here for the case of low-density single-molecule data. Additionally, the SMALL-LABS algorithm is modular, and we encourage users to incorporate it into their own code, for instance in order to use different detection, analysis, or filtering tools than the ones we provide. For example, researchers imaging high-density fluorophores will need to modify several parts of our code, or use their own code, to implement the SMALL-LABS algorithm for background removal. Specifically, in the high-density case, where there are many in-frame overlapping molecule PSFs, our method here of determining "off" frames (Step *III*) will need to be modified. We show here that, for a range of experimental conditions and desired measurements, SMALL-LABS successfully detects single molecules and accurately estimates the background to reduce biases due to background subtraction and thereby increase the accuracy of single-molecule position and brightness estimations.

The workflow for the SMALL-LABS algorithm is:

- I. Approximate background subtraction from the raw movie to produce the avgsub movie
- II. Molecule detection in the avgsub movie
- III. "Off" frame identification for each detected molecule
- IV. Accurate background subtraction for each molecule
- V. Further analysis of the true background-subtracted image of each molecule (intensity measurement, position determination, tracking, etc.)

I. Approximate background subtraction

To enable the initial single-molecule detection step (*II*), an approximate background is subtracted from the original movie (the *raw_movie*). This background is only an approximation because the foreground has not been distinguished from the background. The simplest method to calculate the approximate background, which we employ in the provided code, is to calculate a moving temporal mean (or median, or similar statistical measure; Figs. S1, S2, and S3; Tables S1 – S4) for the *raw_movie*. This mean image is shown in Fig. 1 *a*. For simplicity, the example shown in

Fig. 1 calculates an approximate background from the mean of the entire movie. In general, the characteristic on/off frequency of the molecules (from blinking, photobleaching, photoswitching, or motion) should be considered: the choice of the window length over which to calculate an average (or median) should be the longest window possible that does not include slow background changes at lower frequencies than this characteristic frequency. Though the window time is a fairly weak parameter, if this length is too short, fluorophores which do not blink, bleach, or move over the window length will be erroneously removed with the more static background. Having a long window time relative to the characteristic on/off time increases the accuracy of the approximate calculation of the background by minimizing contributions from molecules to the mean. The mean *raw_movie* image is then subtracted from each frame of the *raw_movie* to produce the *avgsub_movie*, the approximate background-subtracted movie (20, 23, 24), as shown in Fig. 1 b.

II. Molecule detection

An obscuring background in the *raw_movie* could produce a large number of false-positive or false-negative errors in single-molecule detection. The approximate background removal in Step *I* allows molecules to be identified in the *avgsub_movie* (Fig. 1 *b*) with standard image analysis techniques. Any suitable detection algorithm can be used for Step *II* in the SMALL-LABS algorithm. For example, the detection algorithm we provide in our code applies a bandpass to the image in spatial frequency, then identifies spots brighter than a user-supplied threshold percentile and that have an equivalent diameter (calculated with *regionprops* in Matlab) near the PSF size.

Though the accuracy and precision of these detections may be hindered by the approximate background (Supplementary Note 2), detecting molecules in the <code>avgsub_movie</code> rather than in the <code>raw_movie</code> greatly reduces the likelihood of false-positive and false-negative detection errors. For example, molecular detection in the <code>raw_movie</code> would likely have missed molecule 3 in Fig. 1 (a false-negative error). Similarly, single-molecule detection in the <code>raw_movie</code> would have incorrectly identified the eyes in the background smiley face in Fig. 1 as molecules, giving several false-positive errors. Doing molecule detection in the <code>avgsub_movie</code> avoids such errors. Furthermore, as long as the false-negative rate is low, a substantial false-positive rate is permissible, and the SMALL-LABS algorithm is largely insensitive to any

accuracy or precision loss in this detection step because Step *IV* below repeats the characterization of each single molecule to provide high accuracy and precision measurements and to allow for further false-positive screening.

III. "Off" frame identification

To accurately calculate the true background, it is essential to exclude the foreground (images of single molecules). For each molecule detected in Step *II*, a local "off" frame list is constructed; this list enumerates all frames in which no molecule was detected in the local region. Since we expect a diffraction-limited single molecule image with a shape given by the microscope PSF, this local region is a box about the molecule position with side length approximately double the PSF width, though the local region can be changed for different imaging conditions like defocus. SMALL-LABS is agnostic to whether the same molecule is on in multiple frames. Rather, the "off" frames list depends only on if any molecule is detected in the same local region in other imaging frames, regardless of whether this molecule is the same molecule fluorescing for sequential frames, a molecule that blinks on and off, or distinct molecules that appear at the same location in different frames. The "off" frames list can be calculated over the entire movie, as in Fig. 1, or for a smaller number of frames based on the window length considerations discussed in Step *I*.

For example, in Fig. 1, molecule 2 (green arrow) appears in frame 2 and is the only molecule ever detected in that local region (green box); the "off" frames list for molecule 2 therefore consists of all the other frames in the movie, i.e., frames [1,3,...,25]. Similarly, molecule 3 (blue arrow in Fig. 1) is only fluorescent in frame 3; its "off" frame list is frames [1,2,4,...,25]. On the other hand, molecules 1 and 4 (Fig. 1) appear in the same local region (yellow and red boxes) in different frames, and thus the "off" frames list is the same for both molecules: this list excludes both the frame in which molecule 1 appears and the frame in which molecule 4 appears (Fig. 1 c).

IV. Accurate background subtraction

In this key step of SMALL-LABS, the true background is calculated by taking the temporal mean (or median or similar statistical measure) over only frames in the "off" frame list of the

raw_movie in the local region around a molecule detection (dashed boxes in Fig. 1 c). Whereas an approximate background is removed in Step I and non-specific spatial bandpassing can be used to suppress some backgrounds in Step II, the true background is subtracted here in Step IV. This accurate background does not contain partial images of the molecule itself or of any other molecule (the foreground). This accurate background is subtracted from the original raw_movie image of the molecule (solid boxes in Fig. 1 c) to produce to a local background-free image of the molecule (m₁, m₂, m₃, and m₄ in Fig. 1 c). For example, for molecule 3 (Fig. 1 c), the local region around the molecule is averaged over frames [1,2,4,...,25] to produce the true background, which is subtracted from the image of molecule 3 in the raw_movie frame 3, thereby completely removing the background from the smiley face mouth.

V. Further single-molecule analysis

Once the background has been accurately removed, any further single molecule analysis can be performed. For instance, PSF-fitting the background-free single-molecule image provides super-resolution localization (1–3, 25) while avoiding any biases that could be introduced by the background or by an inaccurate background removal. We discuss these biases in depth in Supplementary Note 2. Importantly, though an approximate background removal like that in Step *I* typically preserves the localization precision for very sparse samples, SMALL-LABS is essential for providing unbiased measurements of single-molecule intensities. Thus, in addition to enabling precise position determination, the emission intensity of each fluorescent molecule can be accurately measured based on PSF fitting or by summing pixel intensities after accurate background subtraction.

Validating SMALL-LABS with simulated data. To test the scope and performance of SMALL-LABS, we simulated realistic single-molecule data with increasingly difficult realistic backgrounds and compared the measured results from the algorithm to the ground truth input to the simulations. Three different simulated movies were analyzed. The first movie (Fig. 2 *a*) has only the simple intensity offset background (nonzero dark counts) common to most electron-multiplying charge coupled device (EMCCD) and scientific complementary metal-oxide-semiconductor (sCMOS) cameras. In addition to the constant intensity offset of Fig. 2 *a*, the

second movie (Fig. 2 b) has several static bright background spots identical to fluorophore images in brightness and size, but invariant over time. This background condition is common when fiduciary markers or photoluminescent nanoparticles (NPs) are incorporated into a sample (22, 26, 27). The third movie (Fig. 2 c) contains the same background as in Fig. 2 b, and additionally has a wide, bright Gaussian image overlaid on the entire movie to mimic the spatially varying background that can result from spatial variations in the excitation laser beam.

The simulated movies were created with signal intensity distributions and noise parameters that realistically occur in single-molecule experiments with fluorescent probes detected on an EMCCD detector (20). The purpose of this dataset is to test the background removal ability of SMALL-LABS and not to push the algorithm to find extremely low signal-tonoise ratio (SNR) molecules or to try to use the algorithm to achieve high-density localization; to analyze such datasets, users will need to modify the code that implements the SMALL-LABS algorithm. Thus, the simulated movies contained reasonable SNRs (here defined as the ratio of the single-molecule fluorescence amplitude to the standard deviation of the movie noise) ranging from 1.25 - 10 (Fig. S7), and localizations were well spatially separated (< 1 molecule/ μ m²) as in standard low-density single-molecule experiments (for instance, single-particle tracking or in vitro single-molecule kinetics). Furthermore, in accordance with experiments, molecules could stay on for multiple frames (the duration of their emission was given by the absolute value of a normal distribution with a mean of one frame and a standard deviation of three frames). Finally, because their location was randomly determined, molecules could appear at the same location as a previous molecule (like molecules 1 and 4 in Fig. 1); in these cases, a simpler algorithm would not remove the background accurately.

As a first measure of performance, we analyzed the ability of SMALL-LABS to accurately detect single molecules. The Jaccard index is the ratio of the cardinality (the number of elements in a set) of the intersection between the set of simulated molecules, S, and the set of detected molecules, D, to the cardinality of the union of S and D (11):

$$Jaccard = \frac{|S \cap D|}{|S \cup D|} = \frac{|S \cap D|}{|S| + |D| - |S \cap D|}$$

The false-positive and false-negative rates, FP and FN, respectively, can be similarly expressed:

$$FP = \frac{|D| - |S \cap D|}{|D|} \qquad FN = \frac{|S| - |S \cap D|}{|S|}$$

The detection results for the simulated molecules (after false-positive filtering of the accurate background-subtracted data in Step V) of the three movies are presented in Table 1. In all three cases, SMALL-LABS performs well, as evidenced by a high Jaccard index and low false-positive and false-negative error rates. In particular, the FP rate does not increase upon addition in Fig. 2 b of the NP background, which is identical in appearance to the molecules. Furthermore, in the case of the laser spot background (Fig. 2 c), molecule detection without background removal would be extremely limited, leading to a substantial increase in the FN rate, whereas most molecules are correctly identified after accurate background subtraction by SMALL-LABS. To illustrate one need addressed by the SMALL-LABS algorithm, we compared the detection results for the comprehensive ThunderSTORM single-molecule image analysis package (28) to the results from our code which implements the SMALL-LABS algorithm (SI Table S5). We find that SMALL-LABS successfully removes the backgrounds in all three cases to significantly reduce the false-positive and false-negative rates relative to ThunderSTORM alone (Supplementary Note 3; SI Figures S4 – S6).

Table 1. Detection Results: Jaccard index, false-positive (FP) error rate, and false-negative (FN) error rate for single molecules in the different simulated movies of Fig. 2.

Background	Jaccard	FP rate	FN rate
dark counts	0.903	0.014	0.086
dark counts + NPs	0.905	0.001	0.089
dark counts + NPs + laser spot	0.878	0.016	0.100

Table 2. Error Distribution Characteristics: mean	$, \mu,$ and standard deviation,	σ , for the simulated
movies.		

movies.			
Background	x position error* (nm)	y position error* (nm)	Intensity error ⁺ (%)
dark counts	$\mu = 0.165$ $\sigma = 13.7$	$\mu = 0.114$ $\sigma = 13.6$	$\mu = 0.821$ $\sigma = 20.6$
dark counts + NPs	$\mu = -0.112$ $\sigma = 13.7$	$\mu = -0.029$ $\sigma = 13.9$	$\mu = 1.12$ $\sigma = 20.5$
dark counts + NPs + laser spot	$\mu = -0.050$ $\sigma = 14.3$	$\mu = -0.185$ $\sigma = 14.4$	$\mu = 1.64$ $\sigma = 21.2$

^{*} x and y position error is the difference between the measured and true positions of the molecule.

In addition to validating the ability of SMALL-LABS to detect molecules (Table 1), we also analyzed the performance of SMALL-LABS in measuring some relevant characteristics of the simulated molecules. Table 2 indicates how accurately SMALL-LABS enables the intensity and super-resolved position (as determined by a least-squares Gaussian fit) of the background-subtracted molecule images of each molecule in each movie to be measured. The mean (μ) and standard deviation (σ) of the error distributions for each measured quantity for all molecules in each movie are tabulated in Table 2. Full distributions and further details are given in Supplementary Note 4. In all three movies, SMALL-LABS performs well (Table 2 and Figs. S8 – S10): all error distributions are centered near μ = 0 and have small σ . Furthermore, the error distributions are fairly insensitive to the nature of the background: there is little change in the statistics between the three movies. Importantly, many approximate background removal approaches introduce a bias ($\mu \neq 0$) in these measured quantities, with especially large biases for intensity measurements (Supplementary Note 2), whereas SMALL-LABS does not introduce any such systematic biases.

Validating SMALL-LABS with live-cell single-molecule tracking. To validate SMALL-LABS and demonstrate its scope, we imaged single fluorescent proteins in living bacteria cells under optimal single-molecule tracking conditions (Fig. 3 *a*, SI Movie S1) and in conditions that preclude traditional single-molecule detection (Fig. 3 *b*, SI Movie S2). We imaged *Bacillus subtilis* strains natively expressing the DNA polymerase PolC fused to the photoactivatable

⁺ The intensity percent error is $\{100\% \times (\text{measured} - \text{true})/\text{true}\}\$ for the summed pixel intensities in the local region around the molecule.

fluorescent protein PAmCherry as the sole source of PolC (strain JWS213). PolC is one of the two replicative DNA polymerases in *B. subtilis* and has been characterized in our previous work (29). To produce the high background in Fig. 3 *b*, a constant 15 W/cm², 488-nm laser illumination generated a strong autofluorescent background in the cells; this background was further complicated by its slow decay over time. By stochastically switching a small subset (1 – 3 molecules per cell) of the PolC-PAmCherry molecules into a fluorescent state at a time (in a single-particle tracking/PALM experiment), we visualized the dynamics of 420 single PolC-PAmCherry molecules in 200 high-background cells (Fig. 3 *b*) and 200 single PolC-PAmCherry molecules in 30 low-background cells (Fig. 3 *a*).

We removed the subtle background from the low-background movies with SMALL-LABS and then analyzed the sub-cellular single-molecules with super-resolution PSF-fitting. The high-background movies were analyzed with the same algorithm. Whereas the background in Fig. 3 b background is sufficiently high to make single-molecule localization essentially impossible in the raw data, after SMALL-LABS background removal, PolC-PAmCherry could be detected in these cells. Both single-molecule localization data sets were then analyzed with the same single-molecule tracking algorithm: trajectories were determined (Fig. 3 c) by optimizing all possible pairings of molecules between consecutive frames using the Hungarian algorithm (30–32). Measured diffusion coefficients for PolC-PAmCherry in the high-background cells matched our previously reported low-background measurements (29) (Supplementary Note 5; Fig. S11). Single-molecule intensities, measured by summing the pixel intensities around each measured molecule, yielded nearly identical distributions in the high- and low-background movies (Fig. 3 d). Both of these results show that SMALL-LABS successfully removed the background from this live-cell imaging experiment without introducing any biases to enable accurate measurements of fluorescence intensity and position in a dataset that would have been impossible to analyze without background removal.

Conclusions. The SMALL-LABS algorithm, with which an arbitrary background is removed from single-molecule imaging data by separating the foreground and the background via local "on" and "off" frame categorization, addresses a gap in many super-resolution imaging packages and enables the detection and localization of single molecules even in the presence of obscuring backgrounds. We have benchmarked the speed of our implementation of SMALL-LABS under a

variety of computer systems and tools (Supplementary Note 6; Table S6). In addition to improving single-molecule localization, SMALL-LABS avoids systematic biases caused by inaccurate background subtraction in measurement of single-molecule intensities. This brightness measurement is a key metric in single-molecule FRET experiments, in single-molecule counting experiments, and as a single-molecule probe of the local environment. The SMALL-LABS data analysis approach requires no changes to experimental methods; in fact, it relaxes experimental constraints: with its improved accuracy and sensitivity, SMALL-LABS opens up many systems previously inaccessible to super-resolution analysis due to difficult backgrounds. Here, we have demonstrated the scope and performance of SMALL-LABS by accurately and precisely measuring simulated data under a variety of realistic background conditions, and by successfully measuring and tracking single fluorescent proteins in a live-cell experiment under conditions that preclude traditional approaches.

ASSOCIATED CONTENT

Supporting Information. Supplementary Discussion Notes 1 - 6, Supporting Tables S1 - S6, Supporting Figures S1 - S11, and Supporting Movies S1 - S2.

Raw Data Availability. Raw datasets of movies of single PolC-PAmCherry molecules in living *Bacillus subtilis* cells with high and low experimental background are provided in uncompressed TIFF format at the University of Michigan's permanent data depository, Deep Blue. https://doi.org/10.7302/Z2CR5RKD.

Code Availability. Open-source Matlab code for implementing SMALL-LABS (GNU General Public License), full documentation, and a quick-start guide with example data is provided (Supplementary Information). Further development and expansion of the code post-publication will be hosted at https://github.com/BiteenMatlab/SMALL-LABS. DOI: 10.5281/zenodo.1438446.

Author Contributions. B.P.I. and J.S.B. designed the research. B.P.I. implemented the SMALL-LABS algorithm, performed the simulated experiments, and analyzed the data. Y.L. performed live-cell imaging and analyzed the data. B.P.I. and S.A.L. wrote the code. All authors

discussed the results. The manuscript was written and edited by all authors. All authors read and approved the manuscript.

ACKNOWLEDGEMENTS

This work was supported by a National Science Foundation award (Grant CHE-1807676) to JSB. BPI was also supported by the National Science Foundation Graduate Research Fellowship Program (grant DGE-1256260). David Rowland provided useful coding guidance. Tiancheng (Curly) Zuo provided helpful feedback during SMALL-LABS development.

FIGURE LEGENDS

FIGURE 1. Schematic illustration of the SMALL-LABS algorithm. (a) Simulated raw data (imaging frames), the mean of the entire movie, and the true background (all on the same grayscale). Frames 1 – 3 have fluorescent molecules, indicated with colored arrows; frames 4 – 25 are identical except for detection noise, and only contain the background; the mean includes a faint image of the real molecules over the true background. (b) Molecule detection in the approximate background-subtracted movie. Solid colored boxes indicate a detected molecule, and dashed colored boxes indicate the local background for that molecule in "off" frames. Box colors correspond to the arrows in a. (c) The SMALL-LABS background subtraction process. The true image of each molecule is obtained by locally subtracting the mean of the "off" frames from the raw image. To see this figure in color, go online.

FIGURE 2. Representative frames from the simulated movies with similar foregrounds and different backgrounds. (a) The background consists of only dark counts. (b) The background contains dark counts and static fluorescent nanoparticles. (c) The movie has dark counts, static fluorescent nanoparticles (NPs), and a spatially varying background. To see this figure in color, go online.

FIGURE 3. Tracking single PolC-PAmCherry molecules in living *Bacillus subtilis* cells. (a) Representative raw-data images of a single PolC-PAmCherry molecule (arrow) in a *B. subtilis* cell; the molecule is easily identifiable and can be tracked over time. (b) No PolC-PAmCherry molecules can be identified by eye in the raw-data images in high-background experimental conditions. (c) Accurate background subtraction with SMALL-LABS enables single-molecules

to be detected and localized from the high-background movie in *b*, and trajectories are obtained (colored lines). (d) Comparison of the measured single-molecule intensities of the fluorescent protein PAmCherry in live-cell movies with low background (white) and with a high background (red) as in *a* and *b*. Scale bars: 1 µm. To see this figure in color, go online.

REFERENCES

- 1. Huang, B., M. Bates, and X. Zhuang. 2009. Super-Resolution Fluorescence Microscopy. *Annu. Rev. Biochem.* 78: 993–1016.
- 2. Thompson, M.A., M.D. Lew, and W.E. Moerner. 2012. Extending Microscopic Resolution with Single-Molecule Imaging and Active Control. *Annu. Rev. Biophys.* 41: 321–342.
- 3. Joo, C., H. Balci, ... T. Ha. 2008. Advances in Single-Molecule Fluorescence Methods for Molecular Biology. *Annu. Rev. Biochem.* 77: 51–76.
- 4. Yu, J. 2016. Single-Molecule Studies in Live Cells. Annu. Rev. Phys. Chem. 67: 565–585.
- 5. Tuson, H.H., and J.S. Biteen. 2015. Unveiling the inner workings of live bacteria using super-resolution microscopy. *Anal. Chem.* 87: 42–63.
- 6. Rust, M.J., M. Bates, and X. Zhuang. 2006. Sub-diffraction-limit imaging by stochastic optical reconstruction microscopy (STORM). *Nat. Methods*. 3: 793–795.
- 7. Betzig, E., G.H. Patterson, ... H.F. Hess. 2006. Imaging intracellular fluorescent proteins at nanometer resolution. *Science*. 313: 1642–1645.
- 8. Hess, S.T., T.P.K. Girirajan, and M.D. Mason. 2006. Ultra-high resolution imaging by fluorescence photoactivation localization microscopy. *Biophys. J.* 91: 4258–4272.
- 9. Sharonov, A., and R.M. Hochstrasser. 2006. Wide-field subdiffraction imaging by accumulated binding of diffusing probes. *Proc. Natl. Acad. Sci.* 103: 18911–18916.
- 10. Small, A., and S. Stahlheber. 2014. Fluorophore localization algorithms for superresolution microscopy. *Nat. Methods*. 11: 267–279.

- 11. Sage, D., H. Kirshner, ... M. Unser. 2015. Quantitative evaluation of software packages for single-molecule localization microscopy. *Nat. Methods*. 12: 717–724.
- 12. Cheezum, M.K., W.F. Walker, and W.H. Guilford. 2001. Quantitative comparison of algorithms for tracking single fluorescent particles. *Biophys. J.* 81: 2378–2388.
- 13. Lee, A., K. Tsekouras, ... S. Pressé. 2017. Unraveling the Thousand Word Picture: An Introduction to Super-Resolution Data Analysis. *Chem. Rev.* 117: 7276–7330.
- 14. Schrimpf, W., A. Barth, ... D.C. Lamb. 2018. PAM: A Framework for Integrated Analysis of Imaging, Single-Molecule, and Ensemble Fluorescence Data. *Biophys. J.* 114: 1518–1528.
- 15. Chen, B.C., W.R. Legant, ... E. Betzig. 2014. Lattice light-sheet microscopy: Imaging molecules to embryos at high spatiotemporal resolution. *Science*. 346: 1257998–1257998.
- 16. Greiss, F., M. Deligiannaki, ... D. Braun. 2016. Single-Molecule Imaging in Living Drosophila Embryos with Reflected Light-Sheet Microscopy. *Biophys. J.* 110: 939–946.
- 17. Tokunaga, M., N. Imamoto, and K. Sakata-Sogawa. 2008. Highly inclined thin illumination enables clear single-molecule imaging in cells. *Nat. Methods*. 5: 159–161.
- Axelrod, D. 1989. Total Internal Reflection Fluorescence Microscopy. *Methods Cell Biol.* 30: 245–270.
- 19. Ha, T., and P. Tinnefeld. 2012. Photophysics of Fluorescent Probes for Single-Molecule Biophysics and Super-Resolution Imaging. *Annu. Rev. Phys. Chem.* 63: 595–617.
- Wertz, E., B.P. Isaacoff, ... J.S. Biteen. 2015. Single-Molecule Super-Resolution Microscopy Reveals How Light Couples to a Plasmonic Nanoantenna on the Nanometer Scale. *Nano Lett.* 15: 2662–2670.
- 21. Willets, K.A., and R.P. Van Duyne. 2007. Localized Surface Plasmon Resonance Spectroscopy and Sensing. *Annu. Rev. Phys. Chem.* 58: 267–297.
- 22. Titus, E.J., and K.A. Willets. 2013. Accuracy of superlocalization imaging using Gaussian and dipole emission point-spread functions for modeling gold nanorod luminescence. *ACS Nano*. 7: 6258–6267.

- 23. Hoogendoorn, E., K.C. Crosby, ... M. Postma. 2014. The fidelity of stochastic single-molecule super-resolution reconstructions critically depends upon robust background estimation. *Sci. Rep.* 4: 3854.
- Donehue, J.E., E. Wertz, ... J.S. Biteen. 2014. Plasmon-Enhanced brightness and photostability from single fluorescent proteins coupled to gold nanorods. *J. Phys. Chem. C.* 118: 15027–15035.
- 25. Thompson, R.E., D.R. Larson, and W.W. Webb. 2002. Precise nanometer localization analysis for individual fluorescent probes. *Biophys. J.* 82: 2775–2783.
- Wertz, E.A., B.P. Isaacoff, and J.S. Biteen. 2016. Wavelength-Dependent Superresolution Images of Dye Molecules Coupled to Plasmonic Nanotriangles. *ACS Photonics*. 3: 1733–1740.
- 27. Carattino, A., M. Caldarola, and M. Orrit. 2018. Gold nanoparticles as absolute nanothermometers. *Nano Lett.* 18: 874–880.
- 28. Ovesný, M., P. Křížek, ... G.M. Hagen. 2014. ThunderSTORM: A comprehensive ImageJ plug-in for PALM and STORM data analysis and super-resolution imaging. *Bioinformatics*. 30: 2389–2390.
- 29. Liao, Y., Y. Li, ... J.S. Biteen. 2016. Single-Molecule DNA Polymerase Dynamics at a Bacterial Replisome in Live Cells. *Biophys. J.* 111: 2562–2569.
- 30. Kuhn, H.W. 1955. The Hungarian method for the assignment problem. In: Naval Research Logistics Quarterly. Wiley Subscription Services, Inc., A Wiley Company. pp. 83–97.
- 31. Liao, Y., J.W. Schroeder, ... J.S. Biteen. 2015. Single-molecule motions and interactions in live cells reveal target search dynamics in mismatch repair. *Proc. Natl. Acad. Sci.* 112: E6898–E6906.
- 32. Rowland, D.J., and J.S. Biteen. 2017. Measuring molecular motions inside single cells with improved analysis of single-particle trajectories. *Chem. Phys. Lett.* 674: 173–178.

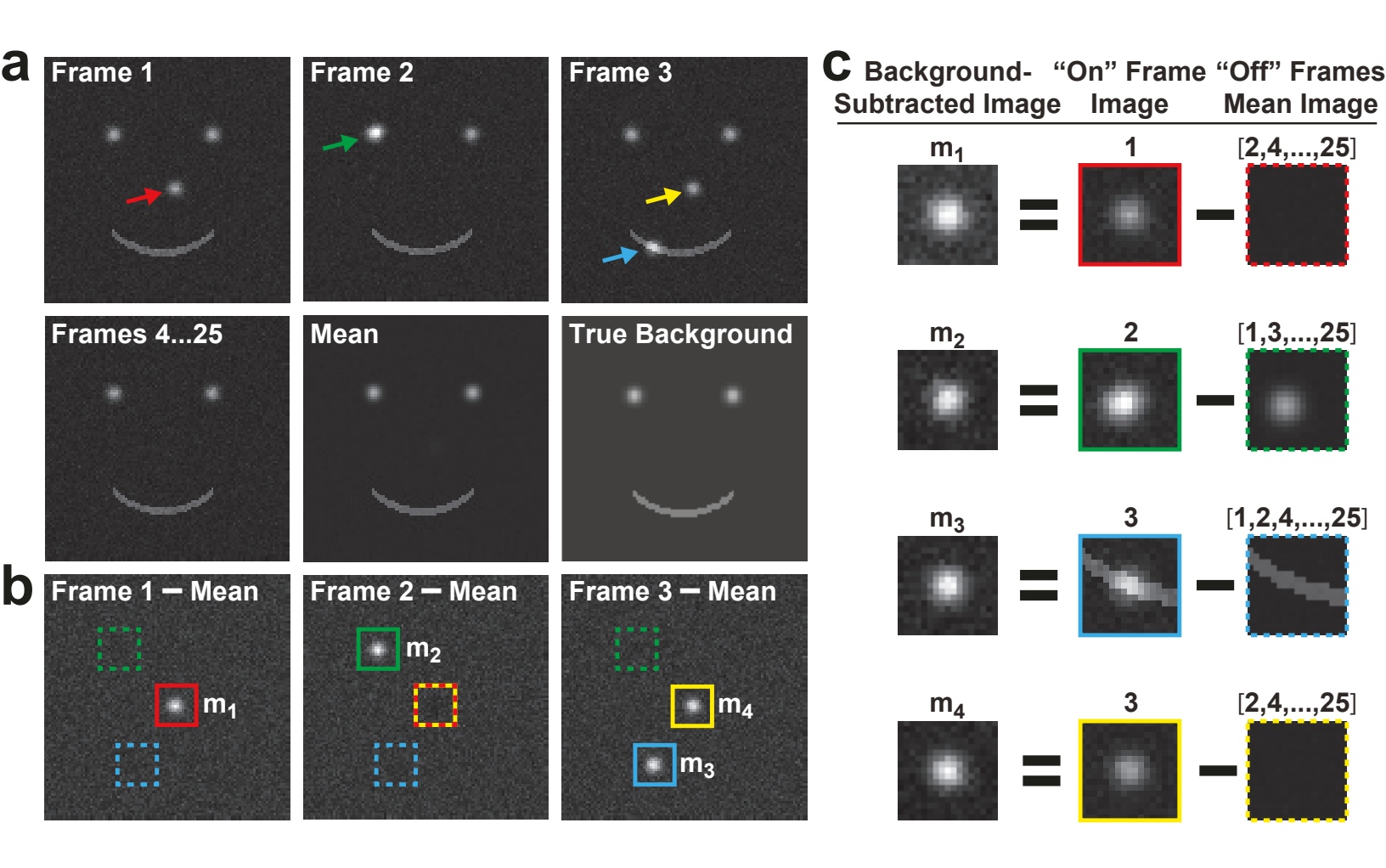


Figure 1

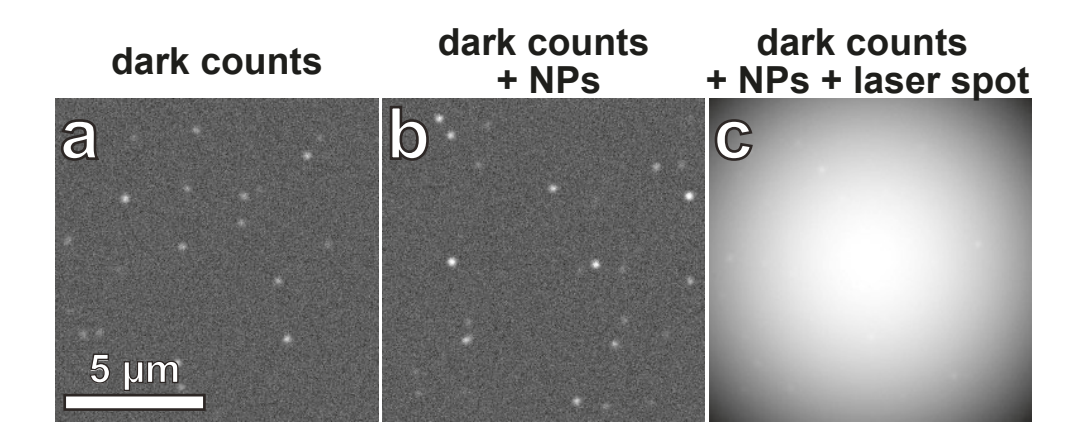


Figure 2

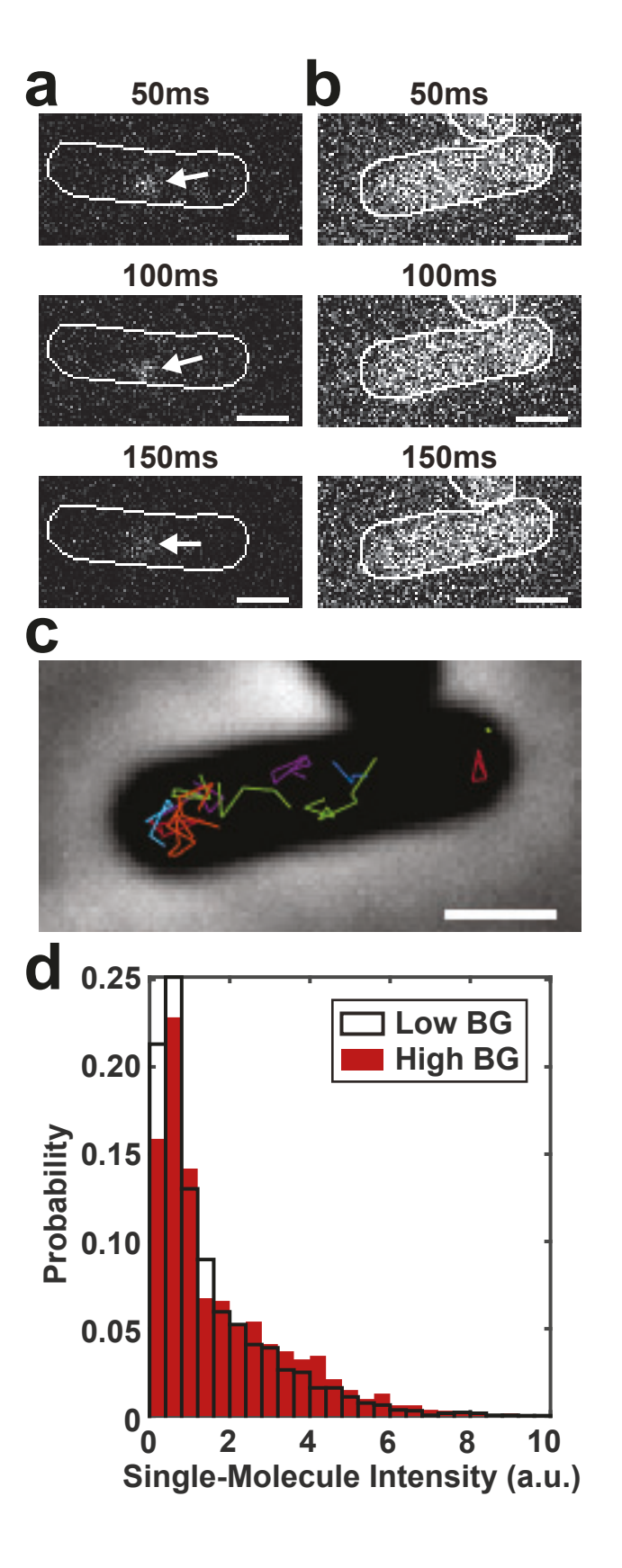


Figure 3

Supplementary Information for: SMALL-LABS: An algorithm for measuring single-molecule intensity and position in the presence of obscuring backgrounds

Benjamin P. Isaacoff, Yilai Li, Stephen A. Lee, and Julie S. Biteen*

University of Michigan Department of Chemistry, Ann Arbor, MI 48104

Contents:

- Supplementary Note 1: Background and context
- Supplementary Note 2: Biases introduced from incorrect background subtraction
- Supplementary Note 3: Comparison to ThunderSTORM
- Supplementary Note 4: Analyzing simulated data with different backgrounds
- Supplementary Note 5: Imaging PolC-PAmCherry in living Bacillus subtilis cells
- Supplementary Note 6: Benchmarking the speed of SMALL-LABS
- Supporting Figures S1 S11
- Supporting Tables S1 S6
- Captions for Supporting Movies S1 S2
- Supplementary References

^{*}To whom correspondence should be addressed: jsbiteen@umich.edu

Supplementary Note 1: Background and context

SMALL-LABS is, to our knowledge, the first general data analysis approach capable of accurately localizing single molecules and measuring their intensity, even in the presence of obscuring backgrounds. In this Supplementary Note, we review other background-removal techniques for single-molecule data to highlight their similarities and differences compared with SMALL-LABS.

SMALL-LABS methodology and advantages

SMALL-LABS localizes single molecules and measures their intensity regardless of the shape or extent of the background. This process is accomplished via three main operations. First, an approximate background removal allows molecules to be detected using standard image analysis techniques. Second, an "off" frame list is constructed; this list enumerates every other frame in which a molecule is not detected in the local vicinity of that detection. Third, the accurate background—an image that contains only "off" frame images and thus no molecules of interest—is specified and removed for each molecule.

The algorithm is very generalizable because it consists of several largely independent modular steps, which allow users to incorporate the most appropriate detection or post-subtraction analysis method (i.e., PALM/STORM, single-molecule tracking, single-molecule intensity measurements, etc.) for their specific application. Furthermore, SMALL-LABS is very flexible: in our code that implements SMALL-LABS, users may specify all parameters. These two points ensure that this algorithm can handle a wide variety of backgrounds, imaging conditions, and experimental modalities. Finally, the only requirement for SMALL-LABS to successfully localize and measure single-molecules is that the local background must change more slowly than the characteristic on/off timescale of the emitting molecules being imaged. Overall, as discussed below, though some of the individual steps of SMALL-LABS are found in the literature, no one approach has put these features together into a cohesive and generalizable algorithm.

(1) Approximate background removal

The first step of SMALL-LABS removes an approximate background to allow single-molecule detection. This initial subtraction is accomplished in SMALL-LABS by subtracting a running temporal mean or median. Though using a mean or a median can sometimes produce different results, they are conceptually very similar; therefore, we do not distinguish between the two operations in the main text. Previously, Hoogendoorn *et al.* subtracted a running temporal median (also referred to as median filtering) (1) and our lab subtracted a running mean (also referred to as mean filtering) (2, 3). Chen *et al.* used box-car blurring to create a background image, which was then subtracted from all frames (4). These techniques provide a good statistical approximation under certain conditions (see Supplementary Note 2). However, when the approximation breaks down due the stochastic nature of single-molecule data, the accuracy and precision of localization and brightness measurements will decrease. Furthermore, given the extreme precision achievable in single-molecule experiments and the deliberate circumvention of ensemble techniques to understand sample heterogeneities, it is essential to detect and accurately measure each and every single molecule. Importantly, SMALL-LABS uses the approximate background subtraction only for this initial molecule detection step.

(2) "Off" frame subtraction only

SMALL-LABS is careful to locally subtract only background frames to leave behind the true foreground. Though this "off" frame subtraction is inspired by precedents in the literature, SMALL-LABS generalizes the concept to arbitrary backgrounds, which may have any shape or brightness and a wide variety of temporal dynamics. In 2014, faced with the challenge of subtracting a specific background—the photoluminescence of a plasmonic nanoparticle—Blythe *et al.* identified "on" frames based on an

expected range of brightnesses for the nanoparticle and the molecules. Then, the specific features of this background were used: the authors fit the average of the "off" frames to a theoretical model of the nanoparticle, then subtracted the nanoparticle fit result from the rest of the frames (5). In their subsequent 2015 work, Blythe *et al.* generalized this approach by subtracting the average image of the "off" frames immediately preceding and following each "on" frame instead of the fit (6). Similarly, Zhou *et al.* addressed a related application—removing the image of a gold nanorod catalyst—by generating the background from a small number of "off" frames preceding each "on" frame (7).

SMALL-LABS increases the signal-to-noise ratio (SNR) of the selective background approach by subtracting *all* local "off" frames (within a user-specified window, to account for instance for a slowly changing background) rather than subtracting only a few frames. Moreover, by defining "on" and "off" in a local area instead of over the full image, SMALL-LABS provides more "off" frames and thus a better estimate of the background. Furthermore, because SMALL-LABS identifies "on" frames with flexible and modifiable molecule detection criteria, the algorithm can be very conservative to minimize the number of false-negative detections which would lead to faulty subtraction (Supplementary Note 2).

In an alternative approach, Zhou et al. identified "on" frames as well as the background intensity level from a 1D time trace (7). Though this approach is perfect for single molecules confined to a specific region—for instance in single-particle catalysis—SMALL-LABS broadens the range of applications by avoiding two main limitations of this 1D signal analysis approach. Firstly, the 1D analysis requires the region of interest (ROI) to be identified *a priori*, whereas SMALL-LABS generalizes the approach to cases in which molecules are detected all over the field of view such that the tail of a given molecule's image might obscure a certain ROI, complicating the statistical analysis. Secondly, SMALL-LABS uses the power of image analysis to identify molecules based on additional pieces of information (size, shape, sparsity, etc.) beyond merely intensity. Furthermore, modern image analysis takes advantage of new algorithms and GPU processors to typically run much faster than serial 1D signal analysis of every pixel in the movie.

(3) Combining an approximate background subtraction with "off" frame identification

In SMALL-LABS, we incorporate and further generalize background subtraction concepts introduced by generalized Single-Molecule High-Resolution Imaging with Photobleaching (gSHRIMP) (8) and Bleaching/Blinking Assisted Localization Microscopy (BALM) (9). The first step of gSHRIMP and BALM removes an approximate background by sequential frame subtraction (frame n' = frame n- frame (n+I)). This initial subtraction was also used by Blythe $et\ al.$ to remove the obscuring background in their experiment before carefully identifying "on" frames (5). The next step in gSHRIMP and BALM identifies when a molecule turns off based on the resulting bright spot in the sequentially subtracted movie. Then these algorithms average groups of frames between sequential turn-off events; this background is subtracted from the detected "on" frames. However, these algorithms are specifically designed for localizing immobile but overlapping and blinking/bleaching fluorophores. If the molecule moves slightly (or changes PSF shape, for instance due to rotation or focus drift) between frames, this kind of subtraction and averaging will reduce the localization accuracy. Here, SMALL-LABS is designed for cases that are more general. SMALL-LABS can handle moving molecules, backgrounds not shaped like molecules, and especially highly obscuring, bright backgrounds. Importantly, the true background in SMALL-LABS is mean (or median) filtered to increase the SNR relative to single background images.

Supplementary Note 2: Biases introduced from incorrect background subtraction

The typical approach to background subtraction is to subtract a temporal mean or median without first doing foreground detection. The assumption in this background subtraction is that because single molecules will only be emissive during a fraction of the temporal window over which the mean or median is calculated, the molecular fluorescence will not contribute significantly to the time-averaged image. However, the fluorescent molecule will contribute some signal, and the magnitude of the single-molecule localization and measurement biases introduced by this approximate background subtraction will increase with the fraction of temporal window during which the molecule fluoresces; this problem scales with the number and density of single molecules.

(1) Avoiding bias in a high density of single molecules

To demonstrate how SMALL-LABS avoids bias (systematic offsets), consider the three-frame movie in Fig. S1a. In this movie, there is an obscuring background blob, and the fluorescent molecule is present in two of the three frames. When the approximate background is calculated based on a three-frame temporal window (Fig. S1b and c), this mean or median filter gives significant biases in localization and intensity metrics. Measurement results for the four cases shown in Fig. S1 are tabulated in Tables S1 and S2. Simply measuring the raw movie produces large errors in all measured quantities. The position, width, and amplitude from a fit of the data to a 2D Gaussian are inaccurate due to the obscuring background. The intensity calculated by summing the pixels is inaccurate due to both the obscuring background blob and the background intensity offset. Note that the ground truth of the sum is not equal to the analytical integral of the 2D Gaussian that was used to simulate the molecules; the volume, V, under a 2D Gaussian curve with these parameters is $V = 2\pi A \sigma^2 = 2513$, whereas the value of 2496 was obtained by summing discrete integer-valued (rounded) pixel intensities in the simulated 2D Gaussian.

In Figs. S1b and c, the mean and median filters qualitatively remove the obscuring background blob and the background intensity offset. However, these filters introduce a new over-correction error by subtracting some intensity from the molecule itself. In this case, where the molecule is fluorescent for a relatively large portion of the filter window time, this over-correction is significant (Tables S1 and S2). The measured intensities, both from the fit amplitude and the sum, are far lower than the ground truth values. Any such over-correction will decrease the measurement precision by decreasing the apparent number of photons measured (10). Furthermore, in the case of a molecule translating between frames (Fig. S1), imperfect subtraction decreases the accuracy and introduces a bias in the measured positions: the apparent position in one frame is pushed away from the location in the other frame. Similarly, in this case of translation where the subtracted molecule is not exactly superposed with the raw molecule image, the result is an error in the measured width. On the other hand, no biases are introduced by SMALL-LABS (Fig. S1d), in which only the "off" frames (in this case frame 3) are subtracted. All measured quantities are measured with high accuracy and precision, closely matching the ground truths.

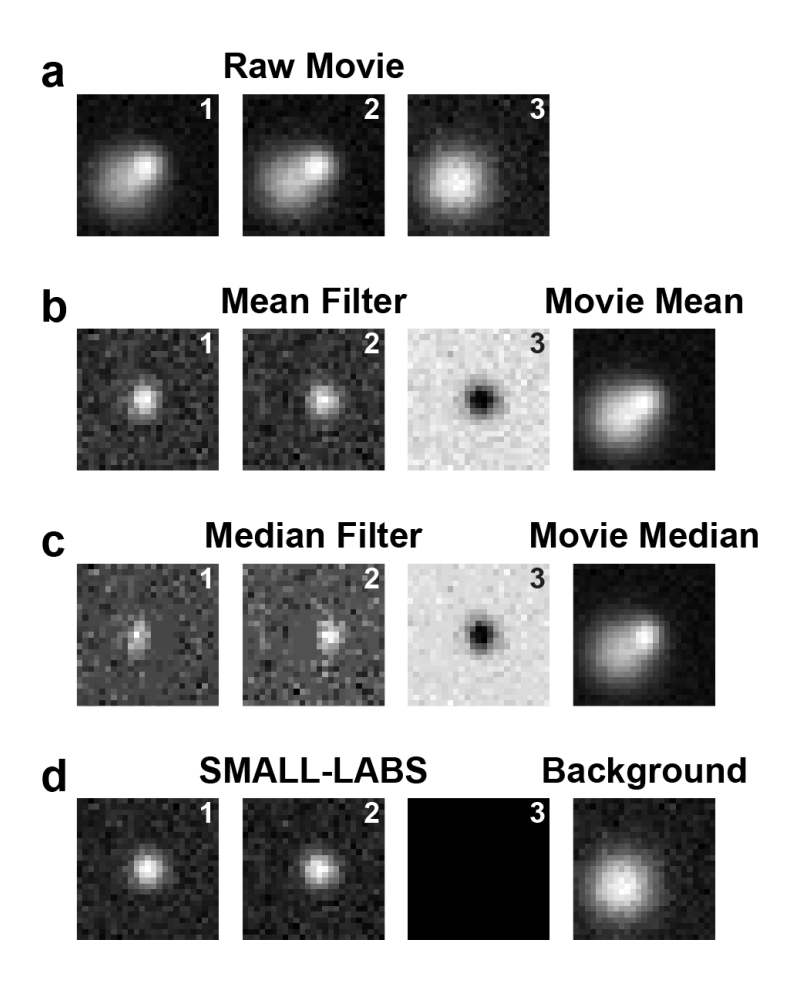


Figure S1: Comparison of different background-subtraction methods for a three-frame movie with a mobile fluorophore; numbers in the top right corners indicate the frame number. **(a)** The raw image frames of the movie. The fluorescent molecule in frame 1 moves to a slightly different position in frame 2 and then photobleaches in frame 3; all frames contain an intensity offset and an obscuring background blob (frame 3). **(b)** Approximate background subtraction by subtracting the movie mean (rightmost panel). **(c)** Approximate background subtraction by subtracting the movie median (rightmost panel). **(d)** True background subtraction using SMALL-LABS, which in this case this is equivalent to subtracting frame 3 in (a) from all frames.

Table S1: Measurements of the position and amplitude of the fluorescent molecule in frame 1 of Fig. S1 based on the background-subtraction approaches in Fig. S1a – d. A 2D Gaussian fit gives the position, width (standard deviation), and amplitude. The sum is the sum of all pixel intensities in the local region around the molecule.

	x position	y position	Width	Fit Amplitude	Sum Intensity
	(px)	(px)	(px)	(a.u.)	(a.u.)
Ground Truth	13.000	13.000	2.00	100.00	2496
(a) Raw Movie	14.298	11.358	3.50	149.81	6.37×10 ⁵
(b) Mean Filter	13.083	12.311	1.89	39.49	800
(c) Median Filter	13.273	11.236	1.63	27.45	451
(d) SMALL-LABS	13.073	13.043	2.00	100.00	2453

Table S2: Measurements of the position and amplitude of the fluorescent molecule in frame 2 of Fig. S1 based on the background-subtraction approaches in Fig. S1a – d. A 2D Gaussian fit gives the position, width (standard deviation), and amplitude. The sum is the sum of all pixel intensities in the local region around the molecule.

	x position	y position	Width	Fit Amplitude	Sum Intensity
	(px)	(px)	(px)	(a.u.)	(a.u.)
Ground Truth	13.000	14.000	2.00	100.00	2496
(a) Raw Movie	14.443	11.778	4.25	148.7	6.37×10 ⁵
(b) Mean Filter	13.138	14.790	1.97	40.15	852
(c) Median Filter	13.198	15.929	1.62	31.09	502
(d) SMALL-LABS	13.100	14.037	2.06	100.36	2504

Though Fig. S1, in which a molecule is on for two frames out of three, seems extreme, this ratio is becoming commonplace as the single-molecule imaging field progresses toward high-density super-resolution imaging by PALM, STORM, or PAINT and toward live-cell imaging of mobile molecules. Overall, detecting one or more fluorescent molecules at different places in the same local region for some number of consecutive frames is not necessarily rare; the likelihood of this occurrence highly depends on the specifics of the imaging and the experimental system. The advantage of SMALL-LABS is that it provides a bias-free measurement regardless of the frequency of occurrence of situations such as Fig. S1, and accurate measurements capable of achieving high precision can always be assured.

(2) Decreased bias in a low density of single molecules

Within the length of the filter window, if the number of "off" frames is much greater than the number of "on" frames, then the bias introduced by approximate background subtraction goes down significantly. To demonstrate this condition, consider a movie (Fig. S2a) which has the same "on" frames as the movie in Fig. S1a, but many more "off" frames (28 rather than just one). In this case, mean and median filtering perform quite well; median filtering gives essentially identical results to accurate background removal using SMALL-LABS. Measurements are tabulated in Tables S3 and S4.

In the limit that the ratio of "on" frames to "off" during the temporal window used for subtraction is small, mean or median filtering perform fairly well. However, this condition is not generally satisfied in single-molecule imaging due to fluorophores remaining "on" for multiple frames, and thus mean or median filtering will in general introduce significant biases. Therefore, the essential benefit of SMALL-LABS is that it does not rely on a potentially difficult-to-satisfy approximation to guarantee *true* background subtraction.

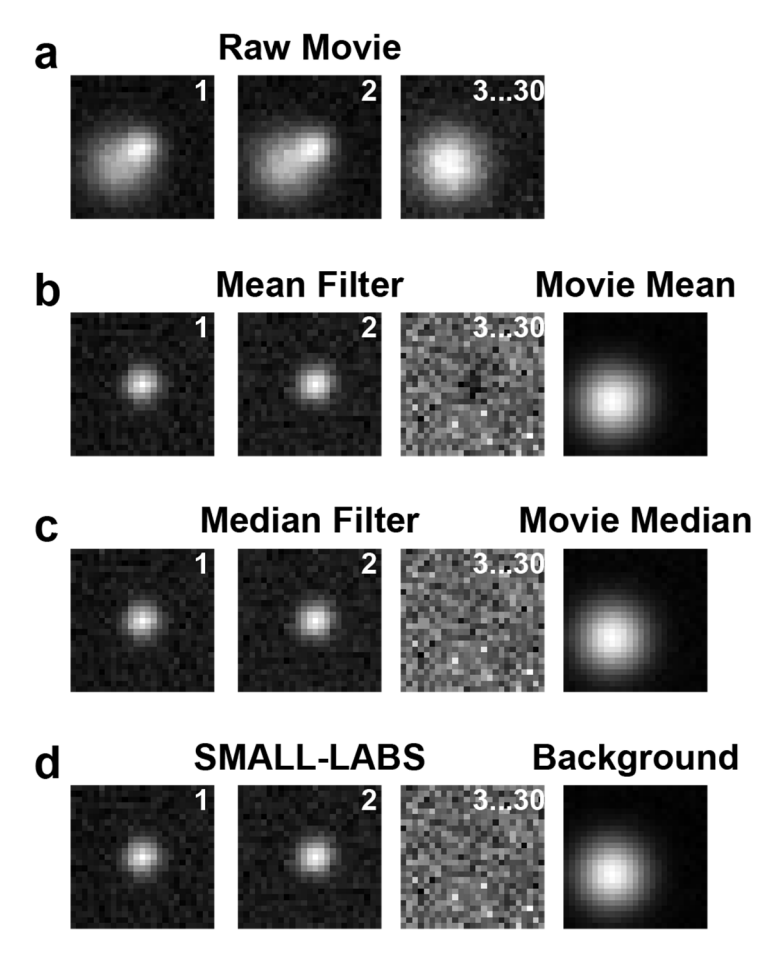


Figure S2: Comparison of different background-subtraction methods for a thirty-frame movie with a mobile fluorophore; numbers in the top right corners indicate the frame number. **(a)** The raw image frames of the movie. The fluorescent molecule in frame 1 moves to a slightly different position in frame 2 and then photobleaches; all frames contain an intensity offset and an obscuring background blob. **(b)** Approximate background subtraction by subtracting the mean of the movie (rightmost panel). **(c)** Approximate background subtraction by subtracting the median of the movie (rightmost panel). **(d)** True background subtraction using SMALL-LABS, which in this case this is equivalent to subtracting the mean of frames 3 to 30 in (a) from all frames.

Table S3: Measurements of the position and amplitude of the fluorescent molecule in frame 1 of Fig. S2 based on the background-subtraction approaches in Fig. S2a – d. A 2D Gaussian fit gives the position, width (standard deviation), and amplitude. The sum is the sum of all pixel intensities in the local region around the molecule.

	x position	y position	Width	Fit Amplitude	Sum Intensity
	(px)	(px)	(px)	(a.u.)	(a.u.)
Ground Truth	13.000	13.000	2.00	100.00	2496
(a) Raw Movie	14.336	11.354	3.48	148.95	6.37×10 ⁵
(b) Mean Filter	13.030	12.990	1.98	93.91	2252
(c) Median Filter	13.027	13.028	1.98	99.70	2390
(d) SMALL-LABS	13.030	13.022	1.99	100.19	2416

Table S4: Measurements of the position and amplitude of the fluorescent molecule in frame 2 of Fig. S2 based on the background-subtraction approaches in Fig. S2a – d. A 2D Gaussian fit gives the position, width (standard deviation), and amplitude. The sum is the sum of all pixel intensities in the local region around the molecule.

	x position (px)	y position (px)	Width (px)	Amplitude (a.u.)	Sum (a.u.)
Ground Truth	13.000	14.000	2.00	100.00	2496
(a) Raw Movie	14.416	11.700	4.04	142.03	6.37×10 ⁵
(b) Mean Filter	13.003	14.009	2.02	93.11	2334
(c) Median Filter	13.002	13.983	2.01	99.06	2472
(d) SMALL-LABS	13.005	13.976	2.02	99.38	2498

(3) Varying the density of single-molecules

The example movies analyzed in sections (1) and (2) above show that SMALL-LABS accurately removes the background and provide bias-free measurements regardless of the density of single-molecules. However, in the low-density case (2), SMALL-LABS does not provide a significant advantage over simple mean or median filtering for most measurables. To demonstrate how the biases introduced by incorrect background subtraction, and consequently the advantage of using SMALL-LABS, scales with the density of molecules, here we analyze the error trends by sweeping the range from the high-density case (1) to the low-density case (2).

The example movies shown in (1) and (2) were simulated with 1 "off" frame and 28 "off" frames, respectively. Here, we held the number of "on" frames at 2 and vary the number of "off" frames from 1 to 28. To statistically sample the errors and account for the simulated noise, each "off" frame case was simulated 1000 times. Each movie was analyzed as described in (1), and the measurement results were compared with the ground truths. The error trends for each measurable are shown in Fig. S3.

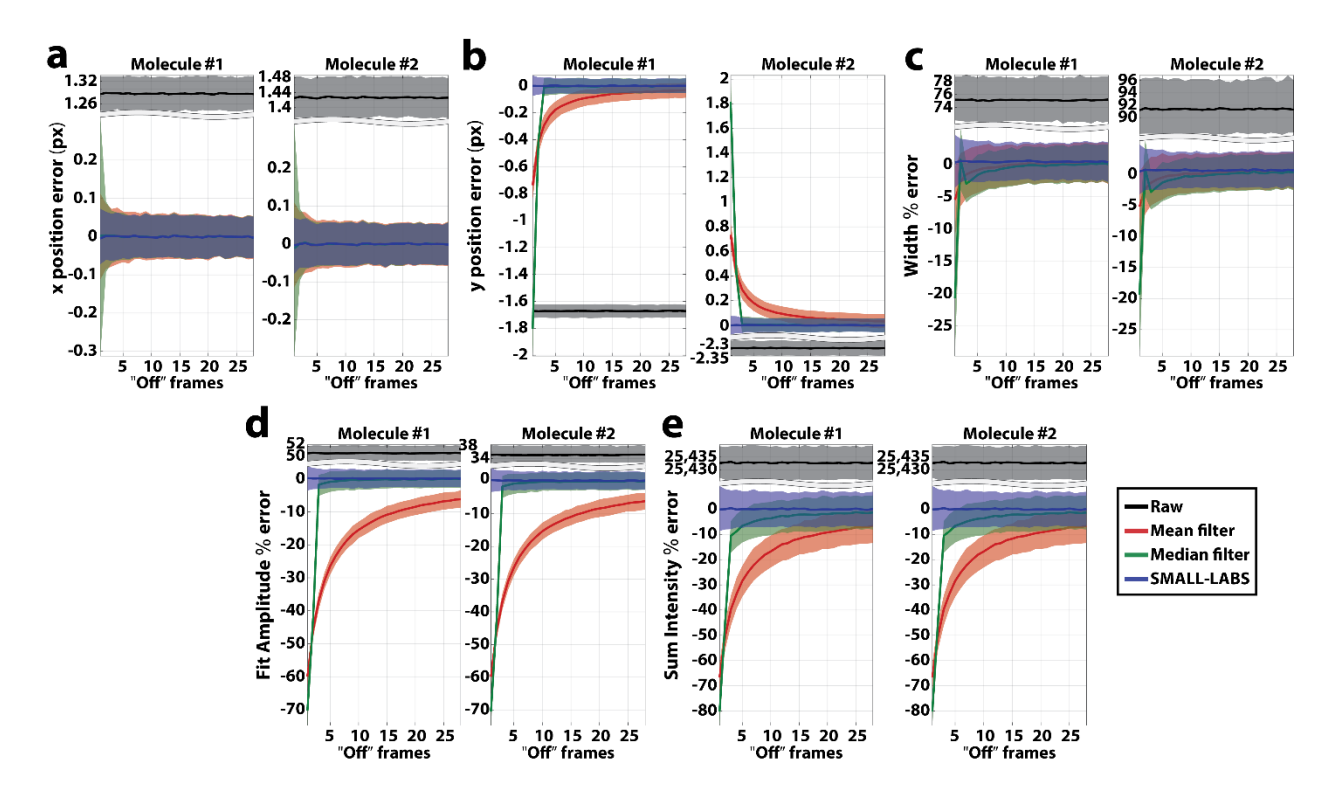


Figure S3: Relationship between single-molecule density and error. The error trends are calculated for a range of conditions from high-density (2 "on" frames and only 1 "off" frames per 30-frame movie) to low-density (2 "on" frames and 28 "off" frames per 30-frame movie). The results for molecule #1 (in frame 1) and molecule #2 (in frame 2) are shown side-by-side. (a) x-position error in pixels. (b) y-position error in pixels. (c) Width percent error. (d) Amplitude percent error. (e) Sum intensity percent error. (a) – (e) black: raw, red: mean filter, green: median filter, blue: SMALL-LABS; the line shown is the median error, and the ribbon edges show the 5th and 95th percentile of the measured errors.

In these movies, the molecule is stationary along the x axis. Accordingly, all background removal approaches similarly remove the background blob and accurately measure the x position (Fig. S3a). However, the molecule translates 1 pixel along the y-axis between frames 1 and 2. Accordingly, for the y position (Fig. S3b), the standard mean filtering never produces a median zero-error result, and the standard median filtering requires more "off" frames than "on" frames to produce an accurate measurement. For the measured width of a fitted 2D Gaussian (Fig. S3c), both mean and median filtering achieve small error, but these approaches require a significant number of "off" frames to produce median zero error. In contrast to these biases for the standard background removal techniques, SMALL-LABS achieves zero median error (blue curves in Fig. S3 a - c) regardless of the number of "off" frames.

For measurements of the molecule intensity, SMALL-LABS provides an even greater comparative advantage. The measured fit amplitude (Fig. S3d) produces large errors for mean and median filtering for a small number of "off" frames. For mean filtering, the median error never reaches zero error for the analyzed number of "off" frames. Median filtering approximately produces the correct measurement only once there are more "off" frames than "on" frames. The preferred measurement of molecule intensity is usually not using the amplitude of a fitted Gaussian (which depends strongly on width and therefore focus), but instead is to use the sum of measured pixel intensities. For the summed intensity (Fig. S3e),

neither mean nor median filtering ever achieve median zero error for the analyzed number of "off" frames; furthermore, both techniques produce very large errors for small numbers of "off" frames. Median filtering does however somewhat quickly achieve small errors.

In contrast to the biases incurred above due to inaccurate background removal techniques, SMALL-LABS achieves zero median error regardless of the number of "off" frames. In particular, if molecule intensity is being measured, then mean or median filtering do not reliably achieve accurate measurements. Furthermore, though mean or median filtering can achieve fairly accurate measurements of position and width in the presence of a sufficiently high number of "off" frames, SMALL-LABS is the only background removal approach capable of *always* achieving accurate measurements of any measurable, regardless of the background or number of "off" frames.

Supplementary Note 3: Comparison to ThunderSTORM

In addition to background subtraction, the SMALL-LABS algorithm improves the detection efficiency of single-molecule localization. To illustrate how SMALL-LABS improves detection, we compared the performance of our open-source code that implements the SMALL-LABS algorithm with the ThunderSTORM data processing package (11). Overall, we find that, despite the simplicity of our open-source code within which SMALL-LABS is implemented, this background-subtraction algorithm serves a need that is not addressed in the state-of-the-art packages to improve the detection efficiency. We therefore propose that even state-of-the-art packages like ThunderSTORM could benefit from the addition of the SMALL-LABS algorithm.

We analyzed the three simulated movies described in the main text (Fig. 2); additional details about these simulated movies are given in Supplementary Note 2. The first movie (Fig. 2a) has only the simple intensity offset background (nonzero dark counts) common to most electron-multiplying charge coupled device (EMCCD) and scientific complementary metal-oxide-semiconductor (sCMOS) cameras. In addition to the constant intensity offset of Fig. 2a, the second movie (Fig. 2b) has several static bright background spots identical to fluorophore images in brightness and size, but invariant over time to represent fiduciary markers or photoluminescent nanoparticles (NPs). The third movie (Fig. 2c) contains the background of Fig. 2b in addition to a wide, bright Gaussian image overlaid on the entire movie to mimic the spatially varying background that can result from spatial variations in the excitation laser beam.

We analyzed each of these movies using ThunderSTORM. For all three movies, we used ThunderSTORM's most advanced pre-processing options: filtering with the *Wavelet filter (B-Spline)* and molecule detection accomplished by locating the *centroid of connected components*. A user-specified threshold is then applied; we used the recommended approach of scaling the std(Wave.F1) metric by a scalar multiplier. The detection results for ThunderSTORM are compared to the results from our code, which implements the SMALL-LABS algorithm shown in Table S5.

Overall, we find that for the cases of interest in this manuscript, SMALL-LABS successfully removes the backgrounds in all three cases to significantly reduce the false-positive and false-negative rates.

Table S5. Comparison to ThunderSTORM detection results: Jaccard index, false-positive (*FP*) error rate, and false-negative (*FN*) error rate for single molecules in the three simulated movies of Fig. 2.

	SMALL-LABS Analysis ⁺		ThunderSTORM Analysis			
Background	Jaccard	FP rate	FN rate	Jaccard	FP rate	FN rate
dark counts	0.903	0.014	0.086	0.788	0.102	0.134
dark counts + NPs	0.905	0.001	0.089	0.595	0.336	0.150
dark counts + NPs + laser spot	0.878	0.016	0.100	0.170	0.700	0.719

^{*}From Table 1

(1) A sparse set of single molecules overlaid with dark-count statistics (Fig. 2a)

In this most simple example, the detection statistics are excellent for both ThunderSTORM and SMALL-LABS. Fig. S4 shows a representative frame of this movie that shows the excellent performance of ThunderSTORM for this case: a single false positive event (red circle toward the bottom) and a single false negative event (blue circle at the top).

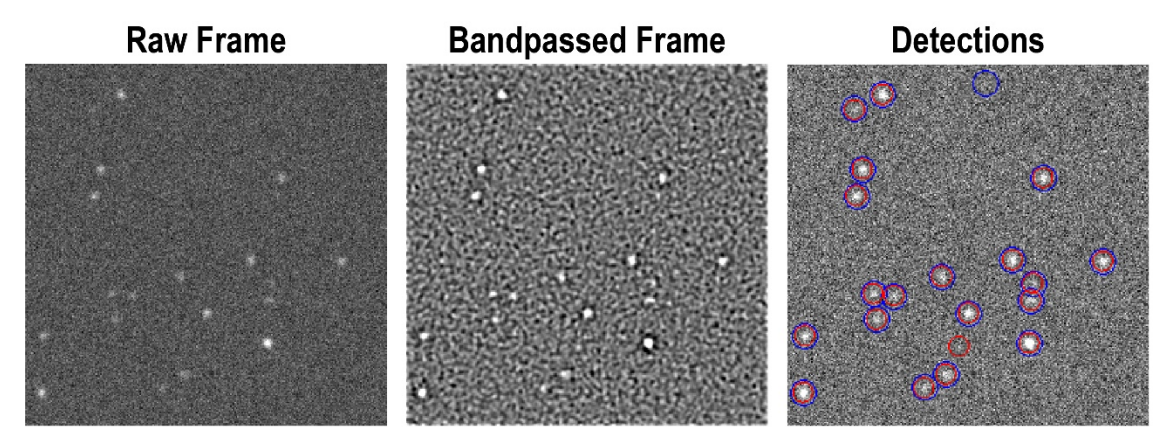


Figure S4: ThunderSTORM analysis of a representative frame in the dark counts movie (Fig. 2a). The bandpassed frame is the result of the preprocessing bandpass filter (calculated with wavelets). The detections are indicated by red circles and the true location of the molecules are indicated by blue circles. Successful detections are denoted by concentric red and blue circles, which may appear pink.

(2) A sparse set of single molecules overlaid with dark-count statistics AND photoluminescent nanoparticles (Fig. 2b)

This movie incorporates several static bright background spots identical to fluorophore images in brightness and size, though invariant over time. This background condition is common when fiduciary markers or photoluminescent nanoparticles (NPs) are incorporated into a sample. Using ThunderSTORM to analyze this movie achieves a low false negative rate. However, ThunderSTORM cannot distinguish between invariant punctate NPs and blinking or photobleaching single molecules, and as a result, it fails

to remove the NP background. In every frame, ThunderSTORM incorrectly identifies the NP background as molecules (green arrows in Fig. S5), leading a significant increase in the <u>false positive rate</u>. Bandpassing an image by any technique does not remove its background.

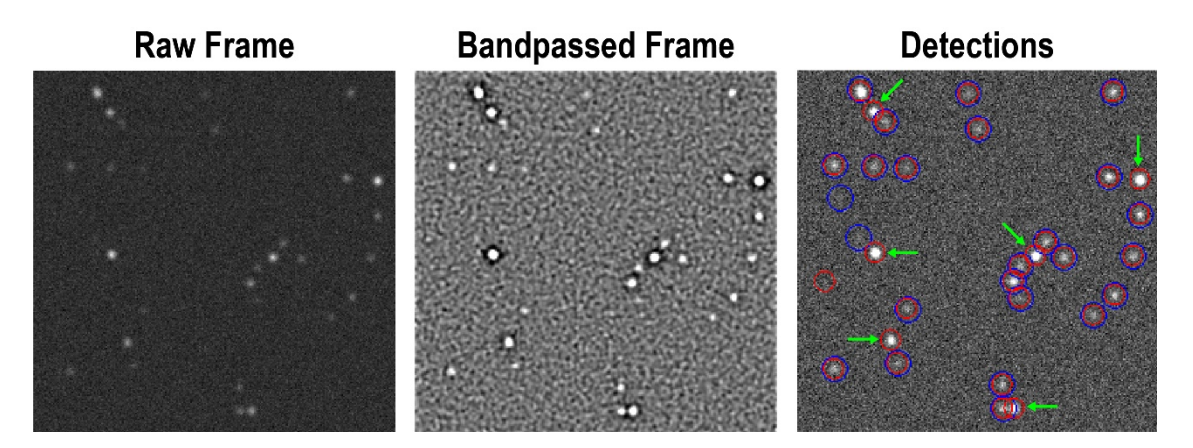


Figure S5: ThunderSTORM analysis of a representative frame in the dark counts + NP movie (Fig. 2b). The bandpassed frame is the result of the preprocessing bandpass filter (calculated with wavelets). The detections are indicated by red circles and the true location of the molecules are indicated by blue circles. Successful detections are denoted by concentric red and blue circles, which may appear pink. The bright spots which come from the temporally static NP background are indicated by green arrows.

(3) A sparse set of single molecules overlaid with dark-count statistics AND photoluminescent nanoparticles AND an uneven background (Fig. 2c)

This movie additionally includes a wide, bright Gaussian image overlaid on the entire movie to mimic the spatially varying background that can result from spatial variations in the excitation laser beam. In this movie ThunderSTORM, fails to detect most of the molecules obscured by the laser spot and gives a very high <u>false negative rate</u> in addition to the high false negative rate in Case 2. These results are shown in Fig. S6.

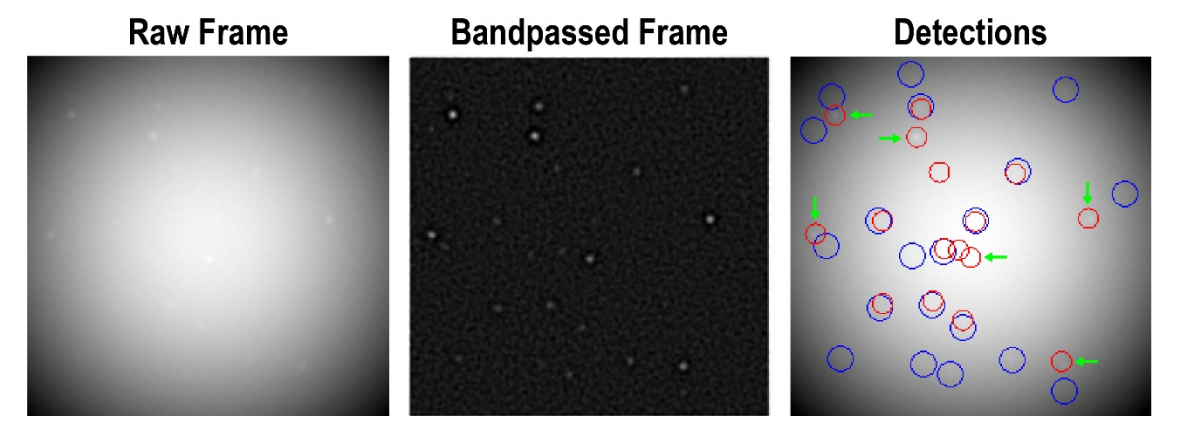


Figure S6: ThunderSTORM analysis of a representative frame in the dark counts + NP + laser sport movie (Fig. 2c). The bandpassed frame is the result of the preprocessing bandpass filter (calculated with wavelets). Successful detections are denoted by concentric red and blue circles, which may appear pink. The bright spots which come from temporally static NP background are indicated by green arrows.

Supplementary Note 4: Analyzing simulated data with different backgrounds

To test the scope and performance of SMALL-LABS, we simulated realistic data with increasingly difficult realistic backgrounds and compared the measured results from the algorithm to the ground truth, as described in the main text. The simulated movies were created with parameters similar to realistic data measured in our lab (3) in a Points Accumulation for Imaging in Nanoscale Topography (PAINT) (12) experiment. The Matlab code used to generate this data is available in the SMALL-LABS GitHub repository under the *Test data and simulations* directory where users can create their own test data matching their experimental setup. The purpose of this simulated data is to show the background removal ability of SMALL-LABS (the purpose of this article) and not to push the algorithm to find extremely low SNR molecules or to try to use the algorithm to do high-density localization, though these functionalities can certainly be incorporated by the user. Thus, the simulated molecules had minimum brightness (Gaussian amplitude) SNR of 1.25, and the data contained no overlapping molecules.

The simulated data uses parameters taken from our experiments on the red dye Cy5 visualized at 20 fps in an epifluorescence microscope with a 1.40-NA $100\times$ objective and a $3\times$ beam expander after the objective; these conditions give a 50-nm pixel width on our Photometrics Evolve electron-multiplying charge-coupled device (EMCCD) detector. The simulated movies have a frame size of 256×256 pixels and are 300 frames long. As is the case for low-brightness optical measurements on an EMCCD camera, the noise was Poissonian (shot noise) for everything except the laser spot itself, which is so bright that it instead has uniformly distributed noise. The intensity offset (dark counts) in all movies is 1040 counts, for which Poissonian noise gives a standard deviation 32.25 counts.

Because most of our experiments are conducted in the red frequency range, each molecule is simulated as a symmetric 2D Gaussian spot with a width (standard deviation) of 100 nm = 2 pixels. The amplitude of the molecules is taken from a normal distribution with a lower bound (Fig. S7). We simulate a PAINT experiment, in which each molecule adsorbs non-specifically onto the coverslip at a random position. The integer number of molecules that appear in each frame is taken from a normal distribution with mean = 1 and standard deviation = 3. In a PAINT experiment, each adsorbed molecule will fluoresce for a finite amount of time before desorbing or photobleaching, the molecule on-times (integer number of frames) are also normally distributed with mean = 3 frames and standard deviation = 7 frames.

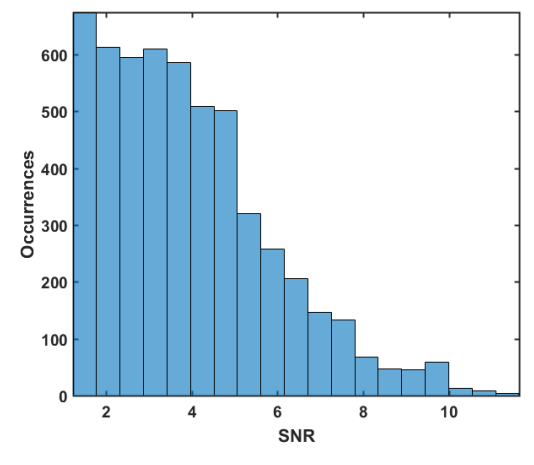


Figure S7: Simulated molecule signal-to-noise ratios (SNRs) in no-background (the dark counts only) movie (Fig. 2a). The SNR is here calculated as the brightness (amplitude of the simulated Gaussian) normalized to the noise standard deviation. The molecule brightnesses in the dark counts + NPs (Fig. 2b) and the dark counts + NPs + laser spot (Fig. 2c) movies followed a similar distribution.

The fluorescent nanoparticle (NP) background (Fig. 2b) was simulated as seven randomly positioned fluorescent spots that were emissive throughout the entire movie. The NP brightnesses were normally distributed with mean = 350 (SNR = 10.9) and standard deviation = 100 (SNR standard deviation = 3.1). The laser spot background (Fig. 2c) was simulated as a Gaussian spot with width (normal distribution standard deviation) of 200 pixels and amplitude of 2×10^4 counts. Because the laser spot is so bright, it falls outside the regime where Poissonian noise is dominant, and instead this background has simple readout noise, which is uniformly distributed from 0 to 200 counts. Representative frames from each movie are shown in Fig. 2.

The movies were analyzed using our open-source code that implements SMALL-LABS. The Matlab function call to run SMALL-LABS to analyze the movies was:

SMALLLABS_main('Documents\SMALL-LABS\Test data and simulations\, 7, 151, 100, 'do_avg', 0, 'do_avgsub', 0, 'bpthrsh', 94.5)

As explained in the User Guide, this function call calculates a running median with a window of 151 frames to do the initial approximate background subtraction. After molecule detection, the accurate background is the median of all the local "off" frames within the surrounding 100 frames. Gaussian PSF fitting then super-resolves the locations of the molecules, and the fit parameters are used in a series of checks to reduce to false positives; molecules that pass this check are called goodfits in the code and the User Guide. The measured results were then compared to the ground truth input into the simulation.

We analyzed the detection results to determine how well a least-squares Gaussian fit of the accurate background-subtracted molecules measured the super-resolved positions of the molecules, their widths (Gaussian standard deviation), and the amplitude of the fitted Gaussian. We also analyzed how well SMALL-LABS measured the integrated fluorescence intensity of the molecule. Here, we show the full error distributions that correspond to the results shown in the main text (Table 2). The results of this analysis are show in Figs. S8 – S10, in which the percent error is:

$$\%$$
 error = $100 \times (true - measured)/true$

Figs. S8 – S10 and Table 2 in the main text show that SMALL-LABS performs quite well in all three cases. The measurement results are generally very accurate and bias-free (centered about mean, μ = 0 error).

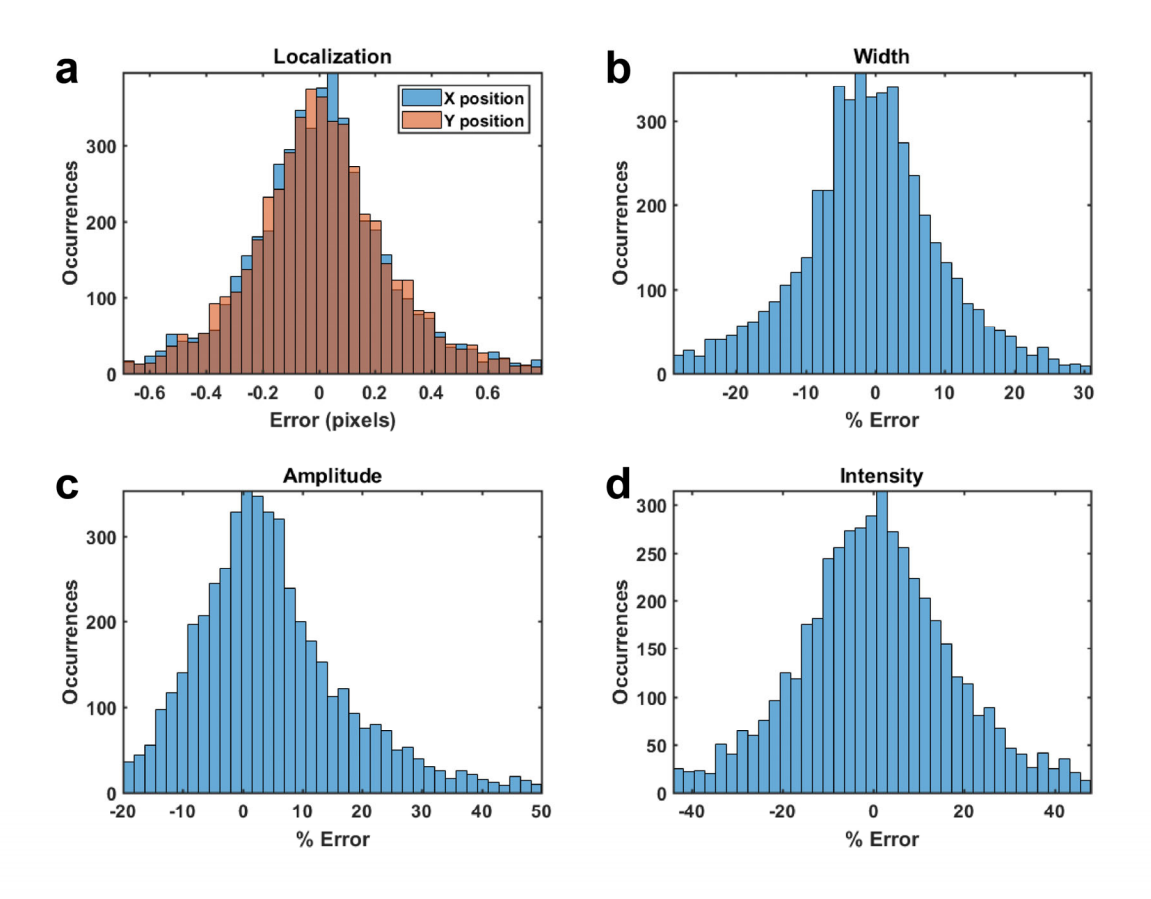


Figure S8: Single-molecule analysis for the dark counts only movie (Fig. 2a). (a) Distribution of the error (in pixels) on the localization (blue: x position, orange: y position). (b) Distribution of the percent error on the width. (c) Distribution of the percent error on the intensity from the fit. (d) Distribution of the percent error on the intensity as measured as the sum of the pixels of the molecule. The mean (μ) and standard deviation (σ) of the error distributions for each measured quantity for all molecules in each movie are tabulated in Table 2.

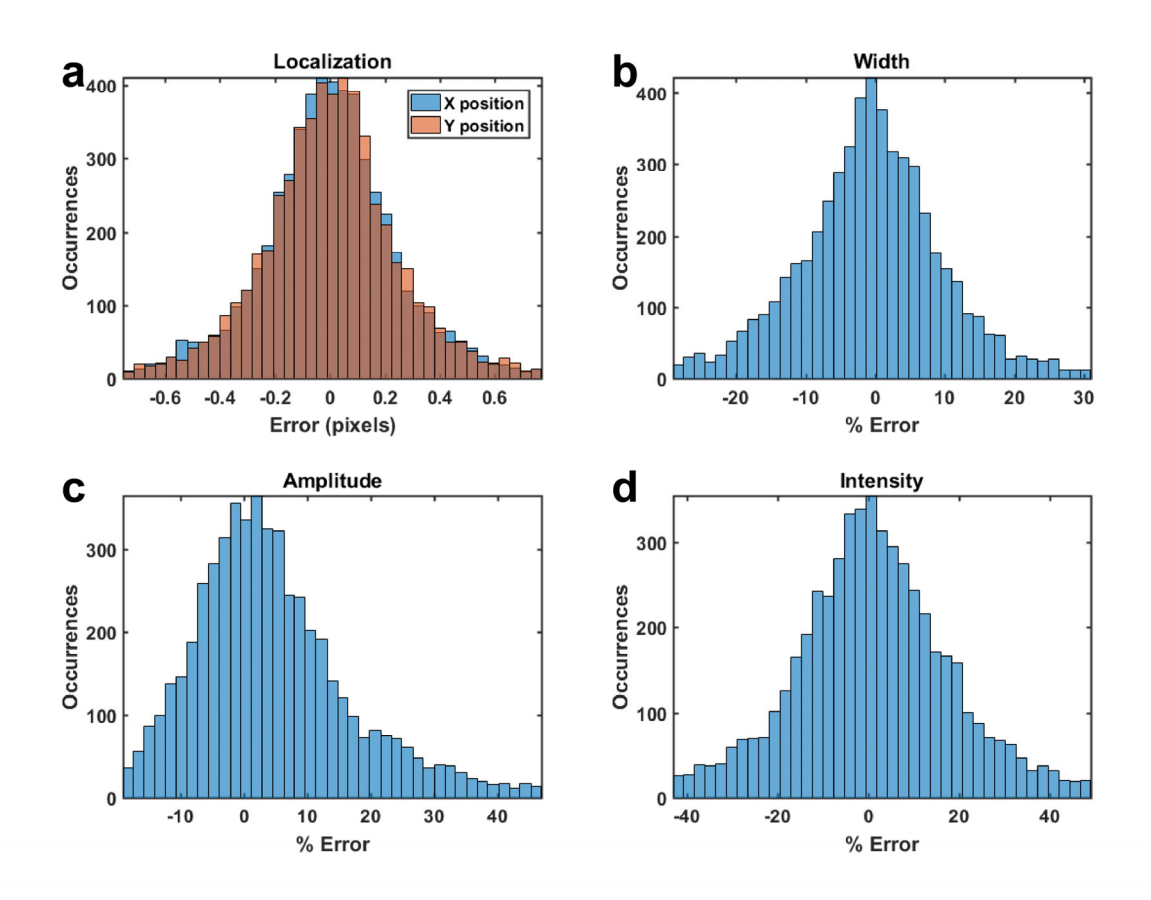


Figure S9: Single-molecule analysis for the dark counts + NPs movie (Fig. 2b). **(a)** Distribution of the error (in pixels) on the localization (blue: x position, orange: y position). **(b)** Distribution of the percent error on the width. **(c)** Distribution of the percent error on the intensity from the fit. **(d)** Distribution of the percent error on the intensity as measured as the sum of the pixels of the molecule. The mean (μ) and standard deviation (σ) of the error distributions for each measured quantity for all molecules in each movie are tabulated in Table 2.

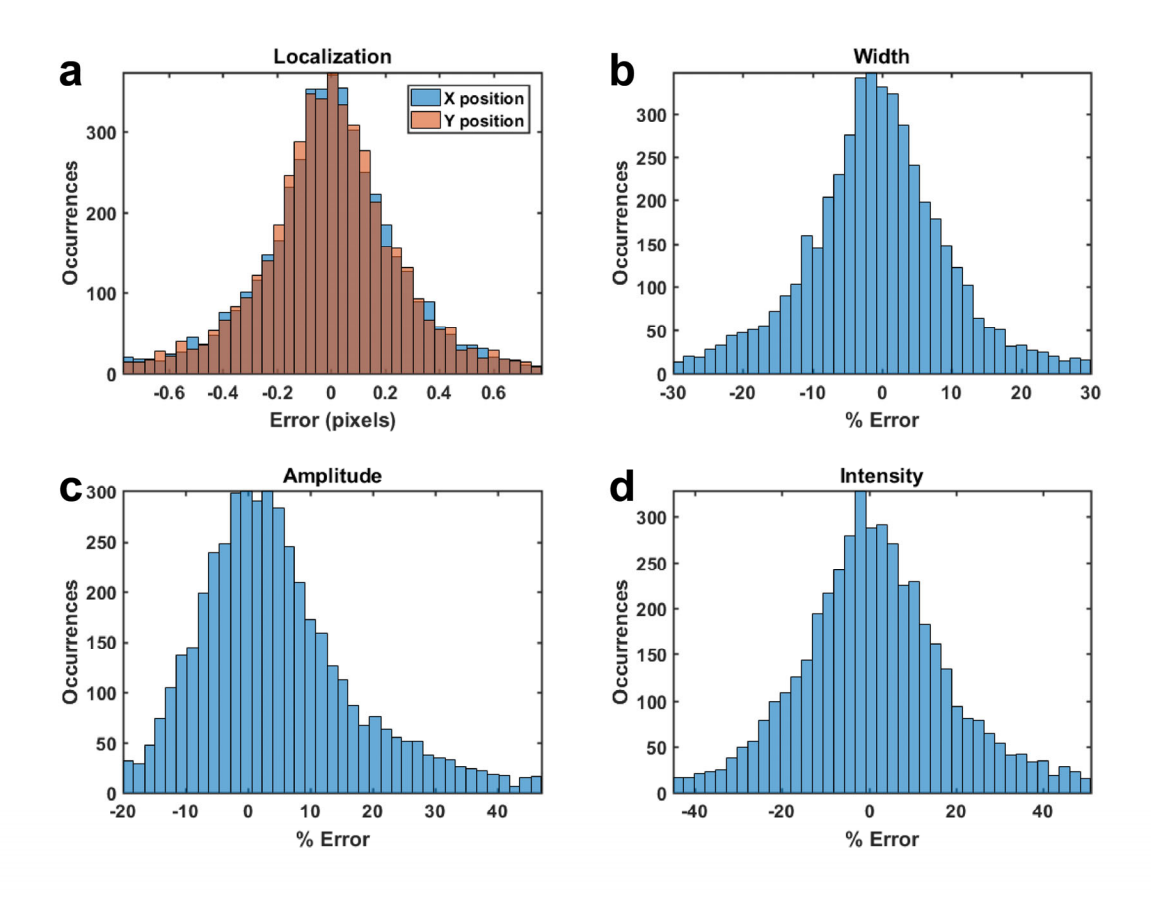


Figure S10: Single-molecule analysis for the dark counts + NPs + laser spot movie (Fig. 2c). **(a)** Distribution of the error (in pixels) on the localization (blue: x position, orange: y position). **(b)** Distribution of the percent error on the width. **(c)** Distribution of the percent error on the intensity from the fit. **(d)** Distribution of the percent error on the intensity as measured as the sum of the pixels of the molecule. The mean (μ) and standard deviation (σ) of the error distributions for each measured quantity for all molecules in each movie are tabulated in Table 2.

Supplementary Note 5: Imaging PolC-PAmCherry in living Bacillus subtilis cells

B. subtilis cells were prepared as previously described (13). Cells were grown at 30 °C to OD \sim 0.55 – 0.65 in S750 minimal medium supplemented with glucose. 2 μL cell culture was pipetted onto a pad of 1% (wt/vol) agarose in S750, which was sandwiched between two coverslips that had been cleaned by oxygen plasma (Plasma Etch PE-50) for 20 min. The sample was then mounted on the microscope for imaging. In both high- and low-background experiments, PAmCherry was photoactivated by a 200-ms pulse of the 405-nm laser (power density: 100 W/cm²; Coherent 405-100) and then imaged with a 561-nm laser (power density: 200 W/cm²; Coherent Sapphire 561-50). The 488-nm laser was not used in the low-background case.

A wide-field inverted microscope (Olympus IX71) was used for imaging, and fluorescence emission was collected by a 1.40-NA 100× oil-immersion phase-contrast objective and detected on a 512×512 pixel EMCCD camera (Photometrics Evolve) at 50 ms/frame. Appropriate dichroic and band-pass filters (Semrock) were placed in the light path to reject scattered laser light and maximize the SNR.

SMALLLABS_main ('DataDirectory', 8, 51, 50, 'do_avg', 0, 'do_avgsub', 0)

This function call uses a running median with a window of 51 frames to do the initial approximate background subtraction. After molecule detection, the accurate background subtraction was calculated as the median of the "off" frames within the surrounding 50 frames. The intensities of the "good fit" molecules from both high- and low-background cells were obtained by summing the pixel intensities in the accurate background-subtracted images of the individual molecules. We observe no significant difference of the intensity distributions in the high and low-background cells (Fig. 3d).

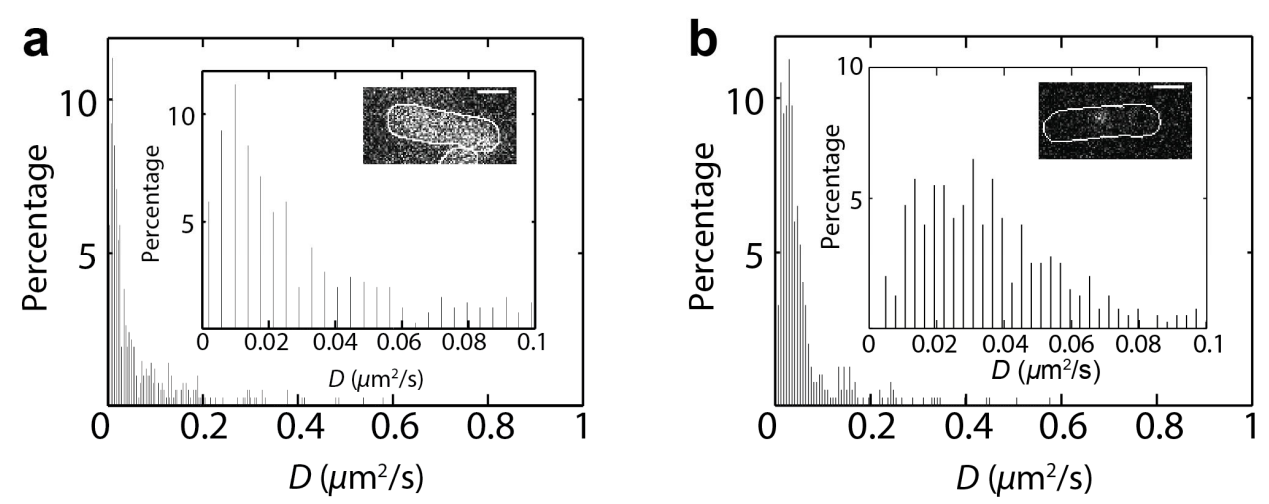


Figure S11: Apparent diffusion coefficients, D, of PolC-PAmCherry in live B. subtilis cells. (a) Distribution of PolC-PAmCherry diffusion coefficients in cells in high-background conditions. (Inset) Zoom-in on the $0-0.1~\mu m^2/s$ region of the histogram and a representative frame showing a high-background image. (b) Adapted from Liao et~al. (13). Distribution of PolC-PAmCherry diffusion coefficients in cells in low-background conditions. (Inset) Zoom-in on the $0-0.1~\mu m^2/s$ region of the histogram and a representative frame showing a low-background image. Scale bars: $1~\mu m$.

High- and low-background data sets were analyzed with the same single-molecule tracking algorithm. The trajectories were determined by optimizing all possible pairings of molecules between consecutive frames using the Hungarian algorithm (14, 15). The likelihood that the two particles are the same molecule in different frames is described in the code by a merit value m (params.trackparams(1) = 0.01), which considers the spatial separation (params.trackparams(4) = 9), the intensity difference, and the temporal separation between the two particles (params.trackparams(3) = 2.5). The sum of m is maximized for each set of adjacent frames and this maximization is repeated until all frames are processed. The apparent diffusion coefficients, D, of single-molecule trajectories were then calculated from the mean squared displacement versus time lag (16). All trajectories at least 5 frames long were analyzed. The distribution of PoIC-PAmCherry diffusion coefficients in high-background cells (Fig. S11a) resembles the distribution characterized in low-background cells (Fig. S11b).

Supplementary Note 6: Benchmarking the speed of SMALL-LABS

The code we provide to implement the SMALL-LABS algorithm is highly modular with a wide range of user options and parameters. Furthermore, the code is open-source and can be updated and improved. Therefore, though the User Guide for the supplied code indicates how various computational methods and parameters are likely to affect the speed, no simple formula can predict how long a given movie will take to analyze with this code.

With these caveats in mind, potential users may wish to get a sense of how fast the code currently runs. To test the speed, we ran a series of benchmarking tests, in which we analyzed three movies with the current version of SMALL-LABS (commit c20943a on GitHub) on three different computers using different computing tools. The movies were made using the same parameters as the tutorial movie supplied with the Quick Start Guide. Briefly, the movies were 100, 1000, and 4000 frames long, respectively. Each movie had on average 17 molecules per frame. The frame size for each movie was 256×256 pixels with 16-bit pixel depth, giving file sizes of 8, 79, and 316 MB, respectively. These movies were loaded from the local hard drive. The three computers used, C1, C2, and C3 are described below:

- C1 Matlab 2017b on Windows 10. Processor: 4x Intel Xeon E5-1620 v4 CPU @ 3.50GHz. Memory: 32 GB DDR4 2400 MHz ECC. Storage: Samsung SSD 850 EVO. GPU: Nvidia GeForce GTX 1070.
- C2 Matlab 2017b on Windows 7. Processor: 4x Intel Core i7-3770 CPU @ 3.40GHz. Memory: 16
 GB DDR3 1330 MHz. Storage: Seagate Barracuda 7200 HDD. No GPU.
- C3 Matlab 2018a on Windows 10. Processor: 2x Intel Core i7-7500U CPU @ 2.70GHz. Memory: 16 GB DDR4 2133 MHz. Storage: Samsung SSD MZNTN. No GPU.

In the current code, SMALL-LABS either uses a graphical processing unit (GPU), runs parallel computations on the main processor, or does the calculations without using Matlab's parallel computing toolbox (PCT) at all. Of the computers tested, only C1 had a CUDA-enabled GPU, and all computers had the PCT installed.

This benchmarking test mostly used the default parameters for processing a batch of movies. The call to SMALL-LABS used was:

SMALLLABS_main ('movie_filename', 7, 500, 100, 'bpthrsh', 96, 'makeViewFits', false)

This command instructs the code to analyze the movie with the SMALL-LABS algorithm, do super-resolution PSF fitting, and track the molecules. As is typical for our batch processing, this command turned off the diagnostic ViewFits movie function, which would add a significant amount of time to the process. Additional details on the numbers and parameters used in this function call can be found in the User Guide.

The results of the benchmarking test are tabulated in Table S6. The results show that for this task and version of SMALL-LABS, using a GPU greatly speeds up analysis. Interestingly, using the PCT does not always speed up the processing, though it usually does.

Table S6. SMALL-LABS benchmarking results for movies of varying lengths run on different computer systems using a range of computing tools.

Computer & setup	100 frame movie	1000 frame movie	4000 frame movie
	runtime (s)	runtime (s)	runtime (s)
C1 w/ GPU	3.9	22	160
C1 w/ PCT w/o GPU	15	88	401
C1 w/o PCT & GPU	32	232	986
C2 w/ PCT	34	277	1,130
C2 w/o PCT	42	257	1,044
C3 w/ PCT	24	140	590
C3 w/o PCT	22	191	796

Conclusion

Because the simulated data is realistic, the results in Supplementary Note 4 demonstrate that SMALL-LABS performs similarly well on real data (for which the ground truth is not known). Taken together with the cellular imaging results presented in Supplementary Note 5, we believe that SMALL-LABS is a powerful tool for localizing and measuring single molecules even in the presence of obscuring backgrounds.

Captions for Supporting Movies S1 – S2

Movie S1. Tracking single PolC-PAmCherry molecules in living *Bacillus subtilis* cells with limited background. Movies are acquired under continuous 561-nm laser excitation at a rate of 40 fps. Scale bar = $1 \mu m$. This movie corresponds to Fig. 3a in the main text.

Movie S2. Tracking single PolC-PAmCherry molecules in living *Bacillus subtilis* cells with a high-background. A constant 15 W/cm², 488-nm laser illumination generated a strong autofluorescent background in the cells. Movies are acquired under continuous 561-nm laser excitation at a rate of 40 fps. Scale bar = $1 \mu m$. This movie corresponds to Fig. 3b in the main text.

The raw, uncompressed data corresponding to Supporting Movies S1 and S2 are provided in uncompressed TIFF format at the University of Michigan's permanent data depository, Deep Blue. https://doi.org/10.7302/Z2CR5RKD

Supplementary References

- 1. Hoogendoorn, E., K.C. Crosby, ... M. Postma. 2014. The fidelity of stochastic single-molecule super-resolution reconstructions critically depends upon robust background estimation. *Sci. Rep.* 4: 3854.
- 2. Donehue, J.E., E. Wertz, ... J.S. Biteen. 2014. Plasmon-Enhanced brightness and photostability from single fluorescent proteins coupled to gold nanorods. *J. Phys. Chem. C.* 118: 15027–15035.
- 3. Wertz, E., B.P. Isaacoff, ... J.S. Biteen. 2015. Single-Molecule Super-Resolution Microscopy Reveals How Light Couples to a Plasmonic Nanoantenna on the Nanometer Scale. *Nano Lett.* 15: 2662–2670.
- 4. Chen, T.Y., A.G. Santiago, ... P. Chen. 2015. Concentration-and chromosome-organization-

- dependent regulator unbinding from DNA for transcription regulation in living cells. *Nat. Commun.* 6: 7445.
- 5. Blythe, K.L., E.J. Titus, and K.A. Willets. 2014. Triplet-state-mediated super-resolution imaging of fluorophore-labeled gold nanorods. *ChemPhysChem.* 15: 784–793.
- 6. Blythe, K.L., E.J. Titus, and K.A. Willets. 2015. Comparing the Accuracy of Reconstructed Image Size in Super-Resolution Imaging of Fluorophore-Labeled Gold Nanorods Using Different Fit Models. *J. Phys. Chem. C.* 119: 19333–19343.
- 7. Zhou, X., N.M. Andoy, ... P. Chen. 2012. Quantitative super-resolution imaging uncovers reactivity patterns on single nanocatalysts. *Nat. Nanotechnol.* 7: 237–241.
- 8. Simonson, P.D., E. Rothenberg, and P.R. Selvin. 2011. Single-molecule-based super-resolution images in the presence of multiple fluorophores. *Nano Lett.* 11: 5090–5096.
- 9. Burnette, D.T., P. Sengupta, ... B. Kachar. 2011. Bleaching/blinking assisted localization microscopy for superresolution imaging using standard fluorescent molecules. *Proc. Natl. Acad. Sci.* 108: 21081–21086.
- 10. Thompson, R.E., D.R. Larson, and W.W. Webb. 2002. Precise nanometer localization analysis for individual fluorescent probes. *Biophys. J.* 82: 2775–2783.
- 11. Ovesný, M., P. Křížek, ... G.M. Hagen. 2014. ThunderSTORM: A comprehensive ImageJ plug-in for PALM and STORM data analysis and super-resolution imaging. *Bioinformatics*. 30: 2389–2390.
- 12. Sharonov, A., and R.M. Hochstrasser. 2006. Wide-field subdiffraction imaging by accumulated binding of diffusing probes. *Proc. Natl. Acad. Sci.* 103: 18911–18916.
- 13. Liao, Y., Y. Li, ... J.S. Biteen. 2016. Single-Molecule DNA Polymerase Dynamics at a Bacterial Replisome in Live Cells. *Biophys. J.* 111: 2562–2569.
- 14. Kuhn, H.W. 1955. The Hungarian method for the assignment problem. In: Naval Research Logistics Quarterly. Wiley Subscription Services, Inc., A Wiley Company. pp. 83–97.
- 15. Liao, Y., J.W. Schroeder, ... J.S. Biteen. 2015. Single-molecule motions and interactions in live cells reveal target search dynamics in mismatch repair. *Proc. Natl. Acad. Sci.* 112: E6898–E6906.
- 16. Saxton, M.J. 1997. Single-particle tracking: The distribution of diffusion coefficients. *Biophys. J.* 72: 1744–1753.